Synthesis of $[(\eta^5\text{-}C_5Me_5)Re(PR_3)_2(p\text{-}N_2C_6H_4OMe)][BF_4]$ (R = Me, OMe), X-ray Crystal Structure of $[(\eta^5\text{-}C_5Me_5)Re(CO)(PMe_3)(p\text{-}N_2C_6H_4OMe)][BF_4]$, and an Investigation of Stereochemical Nonrigidity of a Singly-Bent Aryldiazenido Ligand

Antonio Cusanelli, Raymond J. Batchelor, Frederick W. B. Einstein,* and Derek Sutton*

Department of Chemistry, Simon Fraser University, Burnaby, British Columbia, Canada V5A 1S6

Received July 19, 1994®

The results of an X-ray structural and variable temperature ^1H, $^{13}C\{^1H\}$, and $^{31}P\{^1H\}$ NMR study of the half-sandwich complexes $[(\eta^5\text{-}C_5Me_5)ReL_1L_2(p\text{-}N_2C_6H_4OMe)][BF_4]$ (where (a) $L_1 = L_2 = CO$ **(1)**, PMe_3 **(10)** or $P(OMe)_3$ **(11)** and (b) $L_1 = CO$; $L_2 = PMe_3$ **(3)**, PEt_3 **(4)**, PPh_3 **(5)** (where Ph = C_6H_5), PCy_3 **(6)** (where Cy = C_6H_{11}), $P(OMe)_3$ **(7)**, or PCage **(8)** (where PCage = $P(OCH_2)_3CMe$)) are presented. The new rhenium bis (phosphorus-ligand) complexes **10** and **11** were synthesized by treatment of the cationic bis-acetonitrile complex $[(\eta^5\text{-}C_5Me_5)Re(NCMe)_2(p\text{-}N_2C_6H_4OMe)][BF_4]$ **(9)** with the appropriate phosphine. The $^{31}P\{^1H\}$ NMR spectra of both **10** and **11** showed a single resonance at room temperature which decoalesced into two equal intensity resonances at low temperature, which were assigned to the inequivalent phosphine ligands in the static structure. The $^{31}P\{^1H\}$ variable temperature NMR spectra of **3**, **7**, and **8** also exhibited a single resonance at room temperature which decoalesced into two unequally populated resonances which were assigned to two stereoisomers. The single-crystal X-ray analysis of **3** revealed that this complex crystallizes in the monoclinic space group *Cc* with $Z = 4$, $a = 12.960(2)$ Å, $b = 13.538(2)$ Å, $c = 15.212(3)$ Å, $\beta = 108.59(2)°$, $V = 2529.7$ Å^3 and the structure was refined to $R_F = 0.019$ for 2225 data ($I_o \geq 2.5\sigma(I_o)$) and 266 variables. The most important information provided by the X-ray structure of **3** is the specific orientation of the singly-bent aryldiazenido ligand relative to the other co-ligands. The complex has a ground-state structure in which the aryl ring of the aryldiazenido ligand is oriented towards the carbonyl ligand with a torsion angle with respect to the carbonyl co-ligand, defined by C(carbonyl)-Re--N-C(aryl), of −56.0(4)° while the torsion angle with respect to the trimethylphosphine co-ligand represented by P-Re--N-C(aryl) is −142.6(5)°. Furthermore, both the Re-N-N and the O-C(methoxy) fragments are approximately coplanar with the aryl ring, which suggests a degree of charge delocalization into this ring. Taken together, these results demonstrate that these complexes have ground-state structures in the solid state and in solution in which the aryldiazenido ligand does not orient "symmetrically", i.e., with the NNC (aryl) plane bisecting the L_1ReL_2 angle, but lies "unsymmetrically" with the aryl substituent oriented closer to one of the ligands L_1 or L_2. For the complexes **3**, **7**, and **8** the major isomer was assigned to the conformer where the aryldiazenido ligand is oriented towards the carbonyl ligand. This assignment is in agreement with the molecular conformation observed in the crystal for **3** and with the observed relative differences in the major:minor isomer ratios for complexes **3**, **7**, and **8** which are seen to reflect the differing steric properties of the phosphorus ligands. The minor isomer is assigned a structure in which the aryl ring is oriented towards the phosphine ligand. Interconversion between these structures takes place by a conformational isomerization of the aryldiazenido ligand. Thus, compounds of type (a), where $L_1 = L_2$, i.e., **10** and **11** are 1:1 mixtures of the two possible enantiomers while those of type (b), where $L_1 \neq L_2$, are in the case of **3**, **7**, and **8** mixtures of the two possible diastereomers along with their corresponding enantiomers arising from chirality at Re. The barriers to interconversion of the enantiomers in (a) or diastereomers in (b) were measured and the possible mechanisms for the reorientation of the stereochemically non-rigid aryldiazenido ligand in these complexes are discussed.

Introduction

With the synthesis of $CpMo(CO)_2(N_2Ph)$[1] in 1964 and $PtCl(N_2Ph)(PEt_3)_2$[2a] in 1965, the field of organodiazenido (N_2R) chemistry was born. Although these complexes were initially considered as novelties, the subsequent synthesis of a wide range of organodiazenido complexes

(1) King, R. B.; Bisnette, M. B. *J. Am. Chem. Soc.* **1964**, *86*, 5694.
(2) (a) Parshall, G. W. *J. Am. Chem. Soc.* **1965**, *87*, 2133. (b) Krogsrud, S.; Ibers, J. A. *Inorg. Chem.* **1975**, *14*, 2298.

® Abstract published in *Advance ACS Abstracts,* November 1, 1994.

0276-7333/94/2313-5096$04.50/0

Chart 1. Valence Bond Descriptions for M–N_2Ar

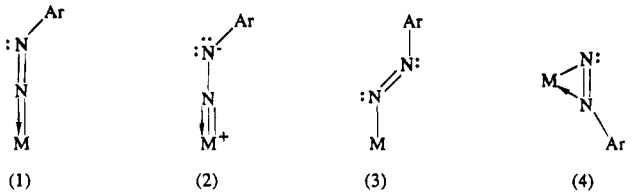

for the majority of the transition metals and the continued investigation of their structural and chemical properties have well established the versatility of organodiazenido ligands in transition metal chemistry.[3] Because of the ready availability of stable aryldiazonium salts as reagents, aryldiazenido (N_2Ar) complexes represent the major class of known organodiazenido compounds. A variety of possible electronic structures and geometries can be visualized for the terminal N_2Ar ligand in a neutral M-N_2Ar situation, and these are described in a simplified fashion by the valence bond descriptions (1) - (4) (Chart 1).

In terms of the number of spectroscopically or X-ray structurally characterized examples, the singly-bent terminal aryldiazenido ligand represented by (1) is by far the most common and well-established for both alkyl (R), and aryl (Ar) substituents; there is little evidence for examples approximating the electron distribution represented by the zwitterion (2). Much less common in transition metal chemistry is the doubly-bent structure (3) even though this is the configuration prevalent in purely organic diazenes such as azobenzene. Currently, (3) is known to be adopted in the crystal structures of $PtCl(p\text{-}N_2C_6H_4F)(PEt_3)_2$[2b], $IrCl_2(o\text{-}N_2C_6H_4NO_2)(CO)(PPh_3)_2$[4] and $[RhCl(triphos)(N_2Ph)]^+$ (where triphos = $PhP(CH_2PPh_2)_2$).[5] Finally, only a single example of the side-on bonded arrangement (4) is known, namely $CpTiCl_2(N_2Ph)$.[6] Exploratory synthesis and product characterization have dominated the first quarter-century of research in transition metal aryldiazenido chemistry in order to establish not only the possible geometric and electronic features of these ligands, but also the metal and co-ligand requirements for forming stable isolable products.

It is worth noting that, despite the large number of structurally characterized examples, there has been, until recently,[7] little attempt to review and discuss the specific orientations adopted by these aryldiazenido ligands in the context of a simple theoretical analysis.[8] For example, in the case of (1), what is the favored orientation of the NNC (aryl) plane of the singly-bent ligand relative to the other co-ligands or the coordinate axes and is the geometry of the complex influenced by the nature of the co-ligands?

(3) For reviews of organodiazenido complexes see: (a) Sutton, D. *Chem. Rev.* **1993**, *93*, 995. (b) Johnson, B. F. G.; Haymore, B. L.; Dilworth, J. R. In *Comprehensive Coordination Chemistry*; Wilkinson, G., Gillard, R. D., McCleverty, J. A., Eds.; Pergamon Press: Oxford, U.K., 1987; Vol. 2, p. 130. (c) Dilworth, J. R. *Coord. Chem. Rev.* **1976**, *21*, 29. (d) Sutton, D. *Chem. Soc. Rev.* **1975**, *4*, 443. (e) Bruce, M. I.; Goodall, B. L. In *The Chemistry of Hydrazo, Azo and Azoxy Groups*; Patai, S., Ed.; Wiley: London, 1975; Part 1, Chapter 9.

(4) Cobbledick, R. E.; Einstein, F. W. B.; Farrell, N.; Gilchrist, A. B.; Sutton, D. *J. Chem. Soc., Dalton Trans.* **1977**, 373.

(5) Gaughan, A. P.; Haymore, B. L.; Ibers, J. A.; Myers, W. H.; Nappier, T. E.; Meek, D. W. *J. Am. Chem. Soc.* **1973**, *95*, 6859.

(6) (a) Dilworth, J. R.; Latham, I. A.; Leigh, G. J.; Huttner, G.; Jibril, I. *J. Chem. Soc., Chem. Commun.* **1983**, 1368. (b) Latham, I. A.; Leigh, G. J.; Huttner, G.; Jibril, I. *J. Chem. Soc., Dalton Trans.* **1986**, 377.

(7) Yan, X. Ph.D. Thesis, Simon Fraser University, 1993.

(8) (a) Dubois, D. L.; Hoffmann, R. *Nouv. J. Chim.* **1977**, *1*, 479. (b) Möller, E. R.; Jorgensen, K. A. *Acta. Chem. Scand.* **1991**, *45*, 68.

Chart 2. Structures of 1–11 (Ar = *p*-C_6H_4OMe)

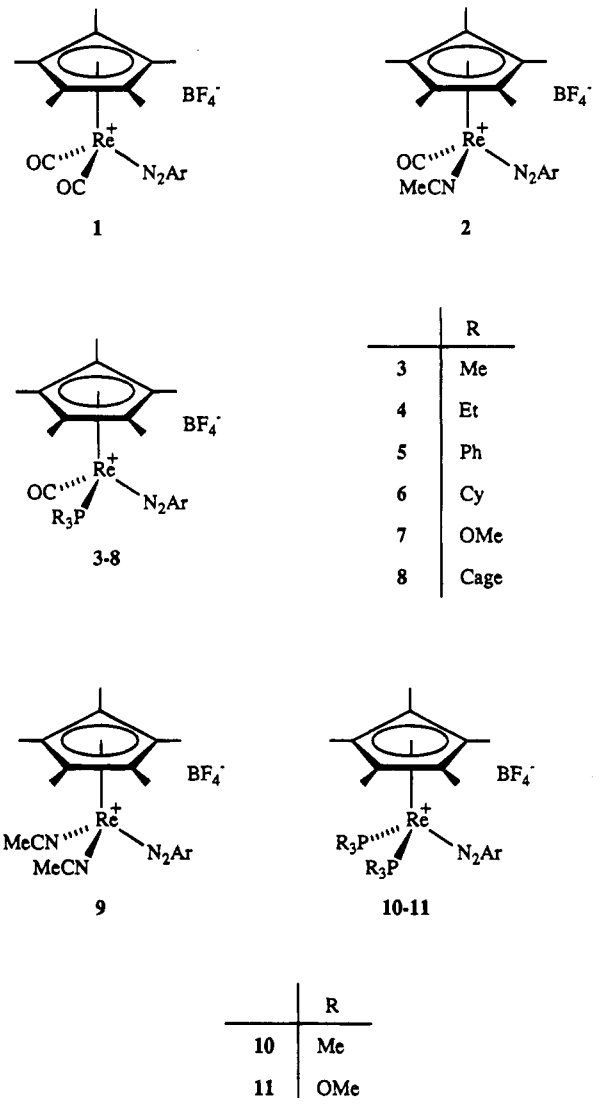

In this paper we report the results of an X-ray structural and variable temperature solution ^{1}H, ^{31}P-{^{1}H} and ^{13}C{^{1}H} NMR study of the half-sandwich complexes $[Cp^*ReL_1L_2(p\text{-}N_2C_6H_4OMe)][BF_4]$ (where $Cp^* = \eta^5\text{-}C_5Me_5$, and (a) $L_1 = L_2 = CO$ (**1**), PMe_3 (**10**) or $P(OMe)_3$ (**11**) and (b) $L_1 = CO$; $L_2 = PMe_3$ (**3**), PEt_3 (**4**), PPh_3 (**5**) (where Ph = C_6H_5), PCy_3 (**6**) (where Cy = C_6H_{11}), $P(OMe)_3$ (**7**), or PCage (**8**) (where PCage = $P(OCH_2)_3CMe$) (Chart 2). We show that these complexes have ground-state structures in the solid state and in solution in which the aryldiazenido ligand does not orient "symmetrically", i.e., with the NNC(aryl) plane bisecting the L_1ReL_2 angle, but lies "unsymmetrically" with the aryl substituent oriented closer to one of the ligands L_1 or L_2; furthermore, interconversion between these structures can take place by a conformational isomerization of the aryldiazenido ligand illustrated schematically in Figure 1. Thus, compounds of type (a), where $L_1 = L_2$, are 1:1 mixtures of the two possible enantiomers while those of type (b), where $L_1 \neq L_2$, are in principle mixtures of the two possible diastereomers along with their corresponding enantiomers arising from chirality at Re. The barriers to interconversion of the enantiomers in (a) or diastereomers in (b) have been measured and the possible mechanisms for the reorientation of the stereochemi-

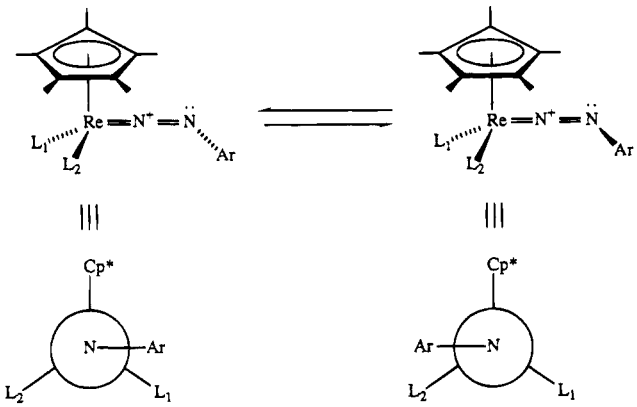

Figure 1. Newman projections of the idealized conformations of the complexes $[Cp^*ReL_1L_2(p\text{-}N_2Ar)]^+$ (Ar = C_6H_4-OMe).

cally non-rigid aryldiazenido ligand in these complexes are discussed.

Experimental Section

General Methods. All manipulations were performed under nitrogen or argon, by using standard Schlenk, drybox or vacuum line techniques unless stated otherwise. Drybox manipulations were carried out in a nitrogen filled Vacuum Atmospheres HE-493 Dri-Lab with attached Dri-Train.

Acetone-d_6 and chloroform-d were obtained from Isotec Inc. All NMR data were recorded at ambient temperatures unless otherwise noted on a Bruker AMX 400 instrument. ^1H and ^{13}C NMR chemical shifts are reported in ppm downfield of tetramethylsilane. ^{31}P NMR chemical shifts are referenced to external 85% H_3PO_4. The terms "virtual doublet" or "virtual triplet" refer to the non-first-order multiplets which are seen in some of the ^1H NMR and $^{13}C\{^1H\}$ NMR spectra; the apparent coupling constant is given by the separation between the two outside peaks.

Infra-red spectra were measured by using a Bomem Michelson model 120 FT-IR instrument, usually as solutions in CaF_2 cells. The IR spectra of the ^{15}N labelled complexes were obtained for 99% ^{15}N isotopically enriched samples. Melting points were determined with a Fisher-Johns melting point apparatus and are uncorrected. All irradiations were carried out using a 200 watt Hanovia high pressure mercury UV lamp at a temperature of 0 °C. All solutions were subjected to a freeze-pump-thaw cycle (2 times) prior to photolysis. Mass spectra were obtained with a Hewlett-Packard Model 5985 mass spectrometer equipped with a fast atom bombardment source (FAB; Phrasor Scientific Inc. accessory, 3-nitrobenzyl alcohol, xenon). Masses are quoted for the ^{187}Re isotope. Microanalyses were performed by the Simon Fraser University Microanalytical Laboratory. X-Ray Fluorescence (XRF) spectroscopy was accomplished with a Kevex Corporation system utilizing a molybdenum secondary target.

Tetrahydrofuran and diethyl ether were distilled from sodium benzophenone ketyl. Hexane was distilled from sodium wire. Acetone was distilled from calcium sulfate. Dichloromethane and acetonitrile were distilled from calcium hydride. All solvents were distilled under nitrogen and used immediately.

Trimethylphosphine (Strem Chemical Co.), trimethylphosphite (Alfa Products, Ventron Division), triphenylphosphine (BDH Chemicals Ltd.), tricyclohexylphosphine (Strem) and triethylphosphine (Aldrich Chemical Co.) were used as purchased and were stored under nitrogen and in the dark. The caged phosphite $P(OCH_2)_3CMe$ was synthesized by the published method.[9] Iodosobenzene was prepared from iodosobenzenediacetate (Aldrich) by the published method[10] and was stored in the refrigerator. Trimethylamine *N*-oxide (Aldrich) was used as purchased and was stored under nitrogen. $(\eta^5\text{-}C_5Me_5)Re(CO)_3$ was synthesized from $Re_2(CO)_{10}$ (Strem) by reaction with pentamethylcyclopentadiene directly.[11] The salt *p*-methoxybenzenediazonium tetrafluoroborate was synthesized by diazotization of *p*-anisidine (Fisher Scientific Co.) with $NaNO_2$ (BDH)[12] or with $Na^{15}NO_2$ (99% ^{15}N; MSD Isotopes Inc.) and was recrystallized from acetone-diethyl ether.

Syntheses. Details have been given in previous publications of the preparation and characterization of $[Cp^*Re(CO)_2(p\text{-}N_2C_6H_4OMe)][BF_4]$ **(1)**,[13] $[Cp^*Re(CO)(NCMe)(p\text{-}N_2C_6H_4OMe)][BF_4]$ **(2)**,[14] and the complexes $[Cp^*Re(CO)(PR_3)(p\text{-}N_2C_6H_4OMe)][BF_4]$ where $PR_3 = PMe_3$ **(3)**, PPh_3 **(5)**, PCy_3 **(6)**, $P(OMe)_3$ **(7)** and PCage **(8)**.[14a] The methods used to prepare these materials in this study were similar. The characterizing spectroscopic data obtained were essentially identical, and additional data have been obtained for some of the compounds. Details for these compounds and the new phosphine complex $[Cp^*Re(CO)(PEt_3)(p\text{-}N_2C_6H_4OMe)][BF_4]$ **(4)** are included as Supplementary Material.

Preparation of $[Cp^*Re(NCMe)_2(p\text{-}N_2C_6H_4OMe)][BF_4]$ (9). Twice the stoichiometric amount of trimethylamine *N*-oxide was added as a solid to a stirred solution of **1** (100 mg, 0.167 mmol) in freshly distilled MeCN (5 mL). (Note: avoid adding a large excess of trimethylamine *N*-oxide since this leads to decomposition of the bis-acetonitrile complex once it is formed). After 30 min all the dicarbonyl complex had reacted to produce **9** as monitored by IR spectroscopy. Removal of solvent under vacuum gave a red oily product which was solidified by washing with diethyl ether (3 times) and dried under vacuum for two days to give **9** as a red-orange solid in 78% yield (81 mg, 0.13 mmol). M.p.: 61–63 °C with decomposition. IR (CH_2Cl_2): 1618, 1588 cm^{-1} [ν(NN) + ν(CC)] (1607, 1578 cm^{-1} for $^{15}N_\alpha$ labeled complex). ^1H NMR (acetone-d_6): δ 1.94 (s, 15H, Cp*), 3.15 (s, 6H, MeCN), 3.83 (s, 3H, OMe), 6.91 (d, 2H, C_6H_4), 7.07 (d, 2H, C_6H_4). $^{13}C\{^1H\}$ NMR (acetone-d_6): δ 4.34 (s, *Me*CN), 9.28 (s, C_5Me_5), 55.53 (s, OMe), 102.86 (s, C_5Me_5), 114.46, 120.39, 123.73, 159.11 (s, C_6H_4), 139.65 (s, Me*C*N). M.S. (FAB, 3-nitrobenzyl alcohol, xenon): m/z 539 (M^+ of cation), 498 (M^+ – MeCN). Anal. Calcd: C, 40.33; H, 4.51; N, 8.96. Found: C, 39.84; H, 4.55; N, 8.77.

Preparation of $[Cp^*Re(PMe_3)_2(p\text{-}N_2C_6H_4OMe)][BF_4]$ (10). A 10-fold stoichiometric excess of PMe_3 was added by syringe to a stirred solution of the bis-acetonitrile complex **9** (100 mg, 0.160 mmol) in acetone (5 mL). An IR spectrum recorded after 24 h indicated that the reaction was complete. No apparent color change was noted. The solvent was removed by vacuum and the remaining oily red-orange product was solidified by washing with diethyl ether (3 times). Recrystallization from acetone-ether gave **10** as a red-orange solid in 72% yield (80 mg, 0.12 mmol). M.p.: 141–143 °C. IR (CH_2Cl_2): 1624, 1591, 1570 cm^{-1} [ν(NN) + ν(CC)] (1611, 1580, 1559 cm^{-1} for $^{15}N_\alpha$ labeled complex). ^1H NMR (acetone-d_6): δ 1.77 (virtual doublet, 18H, PMe_3, J_{app} = 9.0 Hz), 2.11 (s, 15H, Cp*), 3.79 (s, 3H, OMe), 7.03 (s, 4H, C_6H_4). $^{13}C\{^1H\}$ NMR (acetone-d_6): δ 11.65 (s, C_5Me_5), 21.66 (virtual doublet, PMe_3, J_{app} = 37 Hz), 55.98 (s, OMe), 102.81 (s, C_5Me_5), 115.10, 119.54, 122.83, 159.52 (s, C_6H_4). $^{31}P\{^1H\}$ NMR (acetone-d_6): δ –43.28 (s, PMe_3). M.S. (FAB, 3-nitrobenzyl alcohol, xenon): m/z 609 (M^+ of cation), 533 (M^+ - PMe_3). Anal. Calcd: C, 39.72; H, 5.80; N, 4.03. Found: C, 39.56; H, 5.62; N, 4.09.

Preparation of $[Cp^*Re\{P(OMe)_3\}_2(p\text{-}N_2C_6H_4OMe)][BF_4]$ (11). This complex was prepared in a similar manner to complex **10**. The only change made to the procedure was that

(9) Heitsch, C. W.; Verkade, J. G. *Inorg. Chem.* **1962**, *1*, 392.

(10) Saltzman, H.; Sharefkin, J. G. In *Organic Syntheses*; Wiley: New York, 1973; Collect. Vol. V, p 658.

(11) Patton, A. T.; Strouse, C. E.; Knobler, C. B.; Gladysz, J. A. *J. Am. Chem. Soc.* **1983**, *105*, 5804.

(12) Roe, A. In *Organic Reactions*; Adams, R., Ed.; Wiley: New York, 1949; Vol. V, p 193.

(13) Barrientos-Penna, C. F.; Klahn-Oliva, A. H.; Sutton, D. *Organometallics* **1985**, *4*, 367.

(14) (a) Klahn-Oliva, A. H.; Sutton, D. *Organometallics* **1989**, *8*, 198. (b) Barrientos-Penna, C. F.; Gilchrist, A. B.; Klahn-Oliva, A. H.; Hanlan, A. J. L.; Sutton, D. *Organometallics* **1985**, *4*, 478.

Table 1. Rate Constants (k) Derived from Line Shape Analysis

complex	temperature (K)[a]	k (s^{-1})[b]	k (s^{-1})[c]
3	190	6.0 ± 0.2	115 ± 5
	191	7.0 ± 0.2	125 ± 5
	192	8.5 ± 0.5	145 ± 10
	193	10.0 ± 0.5	170 ± 10
	199	25 ± 1	410 ± 25
	210	110 ± 5	1475 ± 75
	223	550 ± 25	5875 ± 300
7	185	9.0 ± 0.5	61.0 ± 2.5
	190	19 ± 1	115 ± 5
	195	38 ± 2	225 ± 10
	197	55 ± 4	340 ± 20
	199	75 ± 5	470 ± 20
	210	325 ± 25	1525 ± 75
	223	1400 ± 100	7100 ± 400
8	188	45.0 ± 2.5	70 ± 5
	190	66 ± 4	95 ± 5
	193	90 ± 5	130 ± 10
	198	250 ± 20	330 ± 30
	203	500 ± 25	670 ± 50
	208	750 ± 50	1100 ± 100
	223	4000 ± 400	5800 ± 500
10	186	135 ± 5	
	190	270 ± 15	
	191	300 ± 20	
	192	400 ± 25	
	193	450 ± 25	
	195	580 ± 30	
	198	860 ± 50	
	203	2000 ± 150	
11	175	975 ± 50	
	180	2200 ± 100	
	185	5100 ± 300	
	190	10000 ± 500	
	195	19000 ± 1000	
	200	30000 ± 2000	

[a] All errors in temperature are ±1 K. [b] For the isomerization process from the more populated to the less populated conformer for complexes **3**, **7**, and **8**. [c] For the isomerization process from the less populated to the more populated conformer for complexes **3**, **7**, and **8**.

upon addition of excess $P(OMe)_3$ the solution was stirred for 72 h in order to complete the reaction. After recrystallization from acetone-ether complex **11** was obtained in 69% yield (87 mg, 0.11 mmol) as a red-orange solid. M.p.: 113–115 °C. IR (CH_2Cl_2): 1640, 1593, 1572 cm^{-1} [ν(NN) + ν(CC)] (1624, 1587, 1566 cm^{-1} for $^{15}N_\alpha$ labeled complex). ^1H NMR (acetone-d_6): δ 2.06 (s, 15H, Cp*), 3.80 (virtual triplet, 18H, $P(OMe)_3$, J_{app} = 11.6 Hz), 3.84 (s, 3H, OMe), 7.07 (d, 2H, C_6H_4), 7.24 (d, 2H, C_6H_4). ^{13}C {^1H} NMR (acetone-d_6): δ 11.67 (s, C_5Me_5), 54.34 (virtual triplet, $P(OMe)_3$, J_{app} = 41 Hz), 55.93 (s, OMe), 109.34 (s, C_5Me_5), 118.32, 120.79, 126.31, 163.34 (s, C_6H_4). ^{31}P {^1H} NMR (acetone-d_6): δ 113.63 (s, $P(OMe)_3$). M.S. (FAB, 3-nitrobenzyl alcohol, xenon): m/z 705 (M^+ of cation). Anal. Calcd: C, 34.90; H, 5.09; N, 3.54. Found: C, 34.81; H, 5.01; N, 3.47.

Variable Temperature NMR and Line Shape Analysis. The variable temperature ^1H, $^{31}P\{^1H\}$ and $^{13}C\{^1H\}$ NMR spectra of complexes **1**, **3–8**, **10** and **11** were recorded at 400, 162 and 100 MHz respectively on a Bruker AMX 400 instrument equipped with a B-VT 1000 variable temperature unit. A cooling unit containing liquid nitrogen and a heater coil was attached to the NMR probe and was used to attain the desired temperature. The NMR sample, in a 5 mm tube, was allowed to equilibrate for 30 min at the desired temperature prior to acquisition of the spectra. A Bruker tunable broad band probe was used to acquire the $^{31}P\{^1H\}$ spectra and a Bruker single frequency probe was used to obtain the $^{13}C\{^1H\}$ spectra. Acetone-d_6 was used as the solvent for all the low-temperature NMR work and spectra were obtained at decreasing temperatures until the solution froze.

Temperatures, which were obtained directly from the VT unit, were checked by measuring peak separations for a standard Bruker sealed sample of methanol and converting these into temperature values using the quadratic equation of Van Geet[15] for methanol. Temperature gradients within the sample region of the AMX 400 spectrometer are considered to be negligible because of the large distance between the cooling unit and the probe; temperatures are accurate to ±1 K. Chemical shifts in the exchange-broadened region were derived from a linear extrapolation[16] of the values obtained at the higher temperatures; this procedure resulted in excellent matching of the experimental and calculated chemical shifts. Linewidths were found to be unchanged at the slow and fast exchange limits and were assumed to be temperature invariant. Calculation of simulated line shapes was performed by use of a slightly modified version of the *DNMR3* program.[17] Rate constants (Table 1) were obtained by visual comparison of the experimental spectra with those calculated for various rates; the errors were considered to be the ranges in rates over which it was impossible to distinguish between the experimental and calculated spectra. Activation parameters and errors were calculated by the use of a linear least-squares program[18] which calculates both Eyring and Arrhenius parameters from an equation of the form $y = a + bx$. Errors in $\Delta G^\ddagger$ values were obtained by use of the following equation[19] for the linearized relative statistical error:

$$(\sigma\Delta G^\ddagger/\Delta G^\ddagger)^2 = [\ln(k_BT/hk)]^{-2}(\sigma_k/k)^2 + \{1 + [\ln(k_BT/hk)]^{-1}\}^2(\sigma_T/T)^2$$

Errors in $\Delta H^\ddagger$, $\Delta S^\ddagger$, E_a and A were obtained from the standard deviations derived from the Eyring and Arrhenius plots multiplied by the appropriate statistical factor.[19]

Crystal Structure of 3. X-ray quality crystals of **3** proved difficult to grow initially as the complex had a tendency to oil out of solution. This problem was overcome by dissolving **3** in a minimum amount of CH_2Cl_2; the solution was then cooled to −78 °C and an excess of hexane was then slowly layered over the CH_2Cl_2 to achieve a distinct solution-solvent interface. The solution was warmed to −10 °C and allowed to intermix for 24 h. At the end of this time, block-like red crystals of **3** suitable for X-ray crystallography had formed.

One of these crystals was mounted in a glass capillary tube using apiezon grease as an adhesive. Data were recorded at ambient temperature with an Enraf Nonius CAD4F diffractometer using graphite monochromatized Mo K_α radiation. Unit cell dimensions were determined from 25 well-centered reflections ($38° \leq 2\theta \leq 44°$). Two intensity standards were measured every hour of exposure time and displayed no significant variations during the course of the measurements. The data were corrected for absorption by the Gaussian integration method and corrections were carefully checked against measured psi-scans. Data reduction included corrections for Lorentz and polarization effects. Crystallographic details are summarized in Table 2.

The structure was solved from the Patterson map by the heavy atom method. After the non-hydrogen atoms were located and refined, an electron density difference map indicated disorder of the expected BF_4^- ion but also a large excess of residual electron density at the boron atom site(s). This can be most reasonably explained by partial substitution of the BF_4^- ion with another anion such as I^- or perhaps ReO_4^-. Iodide was identified as the most reasonable anionic impurity,

(15) Van Geet, A. L. *Anal. Chem.* **1970**, *42*, 679.
(16) Gay, I. D. *LSP*: A computer program which plots linear least-squares polynomials. Simon Fraser University.
(17) Klier, D. A.; Binsch, G. *DNMR3*: A computer program for the calculation of complex exchange-broadened NMR spectra. Modified version for spin systems exhibiting magnetic equivalence or symmetry. Quantum Chemistry Program Exchange, Program 165, Indiana University (1970).
(18) (a) Wolberg, J. R. In *Prediction Analysis*; Van Nostrand: New York, 1967; Chapter 3. (b) Stewart, W. E.; Siddall, T. H. III *Chem. Rev.* **1970**, *70*, 517.
(19) (a) Binsch, G. In *Dynamic Nuclear Magnetic Resonance Spectroscopy*; Jackman, L. M., Cotton, F. A., Eds.; Academic Press: New York, 1975; Chapter 3. (b) Davies, O. L.; Goldsmith, P. L. *Statistical Methods in Research and Production*, Longman: London, 1976; p 438.

Table 2. Crystallographic Data for the Structure Determination of [Cp*Re(CO)(PMe$_3$)(*p*-N$_2$C$_6$H$_4$OMe)][BF$_4$]$_{0.95}$I$_{0.05}$

formula	$ReI_{0.05}PF_{3.8}O_2N_2C_{21}B_{0.95}H_{31}$	crystal system	monoclinic
fw	649.59	space group	*Cc*
a (Å)[a]	12.960(2)	ϱ_c (g cm^{-3})	1.706
b (Å)	13.538(2)	λ (Mo Kα_1) (Å)	0.70930
c (Å)	15.212(3)	μ (Mo Kα) (cm^{-1})	50.3
β (°)	108.59(2)	min-max 2θ (°)	4−50
V (Å^3)	2529.7	transmission[b]	0.340−0.459
Z	4	crystal dim. (mm)	0.28 × 0.32 × 0.34
R_F[c]	0.019	R_{wF}[d]	0.025

[a] Cell dimensions were determined from 25 reflections ($38° \le 2\theta \le 44°$). [b] The data were corrected for the effects of absorption by the Gaussian integration method. [c] $R_F = \sum(||F_o| - |F_c||)/\sum|F_o|$, for 2225 data ($I_o \ge 2.5\sigma(I_o)$). [d] $R_{wF} = [\sum(w(|F_o| - |F_c|)^2/\sum(wF_o^2)]^{1/2}$ for 2225 data ($I_o \ge 2.5\sigma(I_o)$); $w = [\sigma(F_o)^2 + 0.0001F_o^2]^{-1}$.

since it probably arises from PhIO used in the method of preparation and iodine was detected by an X-ray fluorescence (XRF) analysis. A model was developed involving two disordered, rigid BF_4 groups. Each BF_4 group was given a variable occupancy, as were two iodine atoms each of which was constrained to precisely replace each boron atom. The total anionic site occupancy was restrained to 1 and the I/BF_4 occupancy ratios for the two positions were restrained to be equal; the resulting I^- occupancy was 5%. A single isotropic thermal parameter was refined for the boron and iodine atoms and another for the fluorine atoms.

For the cation, anisotropic thermal parameters for all non-hydrogen atoms were included in the refinement, subject to restraints which kept the difference in along-bond thermal motion for bonded atoms to be near zero. Hydrogen atoms were included at calculated positions [d(C−H) = 0.95 Å]. In subsequent cycles of refinement the coordinate shifts for these hydrogen atoms were linked with those for their respectively bound carbon atoms. A single isotropic thermal parameter was refined for: the hydrogen atoms of the Cp* group; those of the PMe_3 group; those on the aromatic ring; and those of the methoxy group.

The correct polarity for the structure was established by refinement (including anomalous contributions to F_c) of a chirality parameter[20] starting from an unbiased model which had previously been refined with exclusion of the anomalous components of the scattering factors. Confirmation of this polarity was obtained by measuring both symmetry equivalent and Friedel non-equivalent reflections for a list of indices predicted to display the most significant Bijvoet differences (R_{merge} = 0.015, for 370 symmetry equivalent pairs). Of the 165 sets of measured Friedel non-equivalents having the largest values of $||F_c + | - |F_c - ||/\sigma(F_o)$ (ranging from 96 down to 7), 164 (including the 163 most significant) displayed the same sign for $|F_o + | - |F_o -|$ as for $|F_c + | - |F_c -|$.

The final full-matrix least squares refinement involved 266 parameters, using 2225 data ($I_o \ge 2.5\sigma(I_o)$) and 28 restraints. An empirical weighting scheme based on counting statistics was applied such that $\langle w(|F_o| - |F_c|)^2 \rangle$ was near constant as a function of both $|F_o|$ and sin θ/λ. The refinement converged at R_F = 0.019 and R_{wF} = 0.025.

Final fractional atomic coordinates for the non-hydrogen atoms are listed in Table 3. The programs used for absorption corrections, data reduction, structure solution and initial refinement, analysis of Bijvoet differences and plot generation were from the *NRCVAX* Crystal Structure System.[21] Refinement was made using *CRYSTALS*.[22] Complex scattering factors for neutral atoms[23] were used in the calculation of structure factors. Computations were carried out on a MicroVAX-II and on 80486-processor-based personal computers.

Table 3. Atomic Coordinates and Equivalent Isotropic Temperature Factors (Å^2) for the Non-Hydrogen Atoms of [Cp*Re(CO)(PMe$_3$)(*p*-N$_2$C$_6$H$_4$OMe)]$^+$

atom	*x/a*	*y/b*	*z/c*	U_{eq}[a]
Re	0.0906(3)[b]	0.12241(2)	0.2512(2)	0.0438
P	−0.0933(3)	0.1406(2)	0.2493(3)	0.0578
O(1)	0.1606(8)	0.2195(5)	0.4432(5)	0.0860
O(2)	0.4368(6)	−0.2673(5)	0.5912(5)	0.0803
N(1)	0.0952(5)	−0.0011(4)	0.2988(4)	0.0472
N(2)	0.0917(6)	−0.0854(5)	0.3239(5)	0.0560
C(1)	0.0582(9)	0.167(1)	0.0987(7)	0.0643
C(2)	0.111(1)	0.2464(6)	0.1559(8)	0.0655
C(3)	0.2152(9)	0.2107(8)	0.2064(6)	0.0640
C(4)	0.2238(9)	0.1115(7)	0.1822(8)	0.0725
C(5)	0.128(1)	0.0849(7)	0.1183(7)	0.0694
C(11)	−0.048(1)	0.175(2)	0.0219(8)	0.1156
C(12)	0.073(2)	0.3528(8)	0.146(1)	0.1166
C(13)	0.304(1)	0.274(2)	0.2676(9)	0.1236
C(14)	0.323(1)	0.049(1)	0.216(1)	0.1193
C(15)	0.112(2)	−0.0119(9)	0.072(1)	0.1246
C(6)	0.1318(8)	0.1838(7)	0.3705(6)	0.0524
C(7)	−0.1506(8)	0.2638(9)	0.234(1)	0.0837
C(8)	−0.112(1)	0.095(1)	0.3549(9)	0.0947
C(9)	−0.1910(9)	0.0658(8)	0.1660(8)	0.0879
C(21)	0.1865(7)	−0.1272(5)	0.3916(6)	0.0517
C(22)	0.1765(8)	−0.2223(6)	0.4232(6)	0.0578
C(23)	0.2590(8)	−0.2646(6)	0.4877(6)	0.0608
C(24)	0.3567(7)	−0.2167(6)	0.5250(6)	0.0567
C(25)	0.3715(7)	−0.1229(6)	0.4920(7)	0.0598
C(26)	0.2857(7)	−0.0780(6)	0.4266(6)	0.0595
C(27)	0.5391(9)	−0.2215(9)	0.6301(8)	0.0872

[a] U_{eq} is the cube root of the product of the principle axes of the thermal ellipsoid. [b] The sums of all x and of all z parameters were restrained to be constants thus fixing the origin in these polar directions. This procedure reduces inter-parameter correlations and produces more realistic coordinate errors.

Results

1. Synthesis of Acetonitrile Complexes 2 and 9. One of the carbonyl groups in [Cp*Re(CO)$_2$(*p*-N$_2$C$_6$H$_4$OMe)][BF_4] (**1**) can be oxidatively removed by reaction with iodosobenzene in the presence of acetonitrile as a solvent to give the mono-substituted acetonitrile complex [Cp*Re(CO)(NCMe)(*p*-N$_2$C$_6$H$_4$OMe)][BF_4] (**2**) in good yield. This method of synthesis was first reported from our laboratory some years ago.[14] Addition of excess iodosobenzene results in the removal of only one carbonyl group. Addition of a large excess of iodosobenzene leads to decomposition of the mono-substituted acetonitrile complex once it is formed and should be avoided. Previously, no success was achieved by using Me_3NO instead of PhIO.[14] However, we now find that **2** can also be made by using a stoichiometric amount of Me_3NO. More importantly, we find that the addition of two equivalents of Me_3NO results in the oxidative removal of both carbonyl groups to give the new bis-acetonitrile complex [Cp*Re(NCMe)$_2$(*p*-N$_2$C$_6$H$_4$OMe)][BF_4] (**9**) in moderate yield. This is feasible since trimethylamine *N*-oxide is a stronger oxidizing agent than iodosobenzene and is soluble in the coordinating solvent acetonitrile, whereas the latter is only sparingly soluble.

The orange and red-orange complexes **2** and **9** are insoluble in hexane or diethyl ether but dissolve in CH_2Cl_2 and acetone. In the IR spectrum of **2** recorded in

(20) Rogers, D. *Acta. Cryst.* **1981**, *A37*, 734.
(21) Gabe, E. J.; Lepage, Y.; Charland, J-P.; Lee, F. L.; White, P. S. *NRCVAX*: An interactive program system for structure analysis. *J. Appl. Cryst.* **1989**, *22*, 384.
(22) Watkin, D. J.; Carruthers, J. R.; Betteridge, P. W. *Crystals*, Chemical Crystallography Laboratory, University of Oxford, Oxford, England, 1984.
(23) International Tables for X-ray Crystallography, Kynoch Press: Birmingham, England (present distributor: Kluwer Academic: Dordrecht, The Netherlands), 1975, IV, 99.

CH_2Cl_2, ν(CO) appeared as a broad, very strong absorption at 1959 cm^{-1} and ν(NN) as a broad, moderately intense absorption at 1658 cm^{-1}. The assignment of ν(NN) was confirmed by ^{15}N isotopic substitution at N_α of the diazenido ligand in the acetonitrile complex [Cp*Re(CO)(NCMe)(*p*-^{15}NNC$_6$H$_4$OMe)][BF_4]. A shift to lower wavenumber by 21 cm^{-1} was then observed. The IR spectrum of **9**, recorded in CH_2Cl_2, displayed a moderate absorption at 1618 cm^{-1} which was assigned to ν(NN). The latter assignment was also confirmed by ^{15}N isotopic substitution at N_α of the diazenido ligand in the bis-acetonitrile complex [Cp*Re(NCMe)$_2$(*p*-^{15}NNC$_6$H$_4$OMe)][BF_4]. A significant shift to lower wavenumber by 11 cm^{-1} was observed. The magnitude of the shift due to isotopic labeling was much smaller for the bis-acetonitrile complex, **9** ($\Delta\nu$ = 11 cm^{-1}), as compared to the mono-acetonitrile complex, **2** ($\Delta\nu$ = 21 cm^{-1}). This result can be accounted for by observing ν(NN) and ν(CC) (aromatic ring stretch) for **2** and **9** for both the isotopically labeled and unlabeled complexes. For unlabeled **2**, ν(NN) and ν(CC) are 1658 and 1590 cm^{-1} respectively. The labeled complex exhibited an isotopic shift to 1637 cm^{-1} for ν(NN) but no appreciable shift for ν(CC). For unlabeled **9**, ν(NN) and ν(CC) are 1618 and 1588 cm^{-1} respectively. The labeled complex exhibited an isotopic shift to 1607 cm^{-1} for ν(NN) and a shift to 1578 cm^{-1} for ν(CC). This result is consistent with assignment of the 1658 cm^{-1} band in **2** as essentially pure ν(NN) but in **9** the 1618 cm^{-1} and 1588 cm^{-1} bands are not pure ν(NN) and ν(CC) but are coupled because of their close proximity. Of note, ν(CN) for the acetonitrile ligand, usually expected to occur quite strongly near 2300 cm^{-1} in the IR spectrum of η^1-bonded acetonitrile complexes, could not be observed in spectra obtained for CH_2Cl_2 solutions or KBr discs for either complex. Other examples of η^1-bonded nitrile complexes with weak or unobserved ν(CN) absorptions have been documented.[24] However, IR spectra obtained during the synthesis of the acetonitrile complexes recorded immediately after the addition of Me_3NO did show a weak band at 2341 cm^{-1}, but this band is assigned not to the coordinated MeCN but to the antisymmetric stretch of carbon dioxide formed during the synthesis, since trimethylamine *N*-oxide acts as a decarbonylating agent and removes CO from the Re complex as CO_2. This assignment was confirmed by bubbling CO_2(g) through acetonitrile for 5 min and then recording an IR spectrum of the resulting solution.

In addition to the typical resonances for the Cp* and aryldiazenido groups, the presence of one and two acetonitrile ligand(s) respectively in **2** and **9** was clearly indicated in the ^1H NMR spectra of these complexes, which exhibited singlet methyl resonances at δ 3.13 and 3.15 which integrated to 3 and 6 protons respectively. In the case of **9** this indicates that the two MeCN ligands are equivalent on the ^1H NMR timescale at room temperature. The $^{13}C\{^1H\}$ NMR chemical shift for the CN carbon(s) of **2** and **9** occurred at δ 143.94 and 139.65 respectively. These values are in agreement with the general region for $^{13}C\{^1H\}$ NMR resonances for comparable cationic MeCN complexes such as [Re(CO)$_5$(NCMe)]$^+$[25] and [CpFe(CO)(NCMe)$_2$]$^+$.[26,27] The FAB mass spectra showed the unfragmented cations as molecular ions M^+, and in each case a fragment corresponding to the loss of the acetonitrile ligand $(M - MeCN)^+$. No fragments were observed corresponding to the loss of CO or the loss of CO and MeCN from **2** or the loss of two MeCN from **9**.

2. Synthesis of carbonyl phosphine and phosphite complexes 3–8. The mono-acetonitrile complex has proven to be a useful precursor to other derivatives where the acetonitrile is substituted by another ligand.[28] For example, phosphines or phosphites can react with **2** to give the corresponding cationic complexes of formula [Cp*Re(CO)(PR$_3$)(*p*-N$_2$C$_6$H$_4$OMe)][BF_4] (**3–8**).[14] These complexes are obtained in good yield by direct addition of the neat phosphine or phosphite to a stirring solution of **2** in acetone at room temperature. In the syntheses conducted for the present study the time required for substitution of the acetonitrile by the respective phosphine or phosphite differed appreciably, with PMe_3 requiring less than an hour to complete the reaction, PEt_3 less than two hours, $P(OMe)_3$, PCage and PCy_3, 4 h and PPh_3, 24 h. (Note: In all cases a 10-fold stoichiometric excess of the phosphorus ligand was added and the reaction was monitored by IR spectroscopy). While no detailed kinetic analysis has been undertaken, this dependence on the phosphine argues against a dissociative mechanism. More probably the substitution reaction may proceed in a concerted fashion, where the Re–P bond is made as the Re–NCMe bond is broken, resulting in a crowded intermediate. If one considers the electronic and steric properties of these phosphorus ligands as quantified by Tolman,[29a] the time required to complete these substitution reactions can be understood. That is, PMe_3 is a very good nucleophile and has a relatively small cone angle (small steric effect) and thus substitution of the acetonitrile ligand proceeds rapidly; PEt_3 is an equally good nucleophile but has a larger cone angle and thus the substitution reaction is slower; $P(OMe)_3$ and PCage are the poorest nucleophiles but have the smallest cone angles while PCy_3 is the best nucleophile but has the largest cone angle and this competing subtle interplay of electronic and steric effects results in an overall longer time to complete the substitution reaction. The substitution reaction is slowest for the PPh_3 ligand since it is a moderate nucleophile but it has a large cone angle.

The characterization of complexes **3**, **5–8** has been described previously[14a] and only brief confirmation and additional observations will be mentioned here. The ^1H NMR spectra exhibited the typical resonances expected for the Cp*, aryldiazenido and phosphorus groups. The only observation of note was that, as observed previously,[14a] the Cp* resonances in **3**, **7** and **8** were split into a doublet with J_{P-H} couplings of 0.5, 0.7 and 0.9 Hz respectively which further substantiated the presence of one phosphorus ligand in the complex. In complexes **4**, **5**, and **6** the Cp* resonance remained a singlet; the expected J_{P-H} couplings are believed to be too small to be observed. The $^{31}P\{^1H\}$ NMR spectra of **3–8**, in each case, showed a single resonance at room

(24) (a) Rouschias, G.; Wilkinson, G. *J. Chem. Soc. A* **1967**, 993. (b) Butcher, A. V.; Chatt, J.; Leigh, G. J.; Richards, P. L. *J. Chem. Soc., Dalton Trans.* **1972**, 1064.
(25) Webb, M. J.; Graham, W. A. G. *J. Organomet. Chem.* **1975**, *93*, 119.
(26) Casey, C. P.; Marder, S. R.; Colbron, R. E.; Goodson, P. A. *Organometallics* **1986**, *5*, 199.
(27) Catheline, D.; Astruc, D. *J. Organomet. Chem.* **1984**, *272*, 417.
(28) Klahn-Oliva, A. H. Ph.D. Thesis, Simon Fraser University, 1986.
(29) (a) Tolman, C. A. *Chem. Rev.* **1977**, *77*, 313. (b) For a published report in support of our steric arguments see: Campion, B. K.; Heyn, R. H.; Tilley, T. D. *J. Chem. Soc., Chem. Commun.* **1988**, 278.

temperature in the normal region for a coordinated phosphine or phosphite. The $^{13}C\{^1H\}$ NMR spectra were recorded for all the complexes **3–8**. It was observed from $^{13}C\{^1H\}$ NMR spectra that replacement of one carbonyl ligand in $[Cp^*Re(CO)_2(p\text{-}N_2C_6H_4OMe)][BF_4]$ by either a phosphine or a phosphite group causes an appreciable downfield shift for the carbon resonance of the remaining CO ligand; the magnitude of the shift is of the order of 12 ppm.[14a] To lend further evidence to phosphorus coordination in these complexes, the $^{13}C\{^1H\}$ NMR spectra also showed that the carbonyl resonance was in each case split into a doublet with a J_{P-C} coupling of 9–12 Hz for the phosphine complexes **3–6** and a J_{P-C} coupling of 17 and 21 Hz respectively for the phosphite complexes **7** and **8**. The parent dicarbonyl complex **1** exhibited only a single signal for $\delta(^{13}CO)$ indicating equivalent CO groups on the NMR timescale at room temperature.[28]

3. Synthesis of Bis(phosphorus-ligand) Complexes 10 and 11. The bis-acetonitrile complex **9** is valuable for the synthesis of derivatives in which both acetonitrile ligands are substituted by other ligands. Addition of 10-fold excess of trimethylphosphine or trimethylphosphite directly to a stirred solution of **9** in acetone at room temperature affords the corresponding cationic complexes of formula $[Cp^*Re(PR_3)_2(p\text{-}N_2C_6H_4OMe)][BF_4]$ **(10)** (R = Me) and **(11)** (R = OMe) in moderate yield. Attempts to synthesize other bis-phosphine complexes (i.e., where $PR_3 = PPh_3$ or PCy_3) by using the same method were not successful. It is believed that this lack of success may be attributed to the large cone angles of these phosphine ligands which make coordination of both phosphines not sterically feasible.[29b] The time required for substitution of both acetonitrile ligands by either PMe_3 or $P(OMe)_3$ differed greatly, with the phosphine ligand requiring less than 24 h to complete the reaction while the phosphite ligand needed nearly 72 h. IR spectra obtained during the course of the reaction indicated a transformation from the bis-acetonitrile complex **9** directly to the corresponding bis (phosphorus-ligand) complexes **10** and **11** as evidenced by the loss of ν(NN) for **9** which was accompanied by the growth of the respective ν(NN) for **10** or **11**. No IR absorption corresponding to the formation of an observable reaction intermediate, such as $[Cp^*Re(PR_3)(NCMe)(p\text{-}N_2C_6H_4OMe)][BF_4]$, was found. Attempts to shorten these reaction times by employing higher temperatures (i.e. refluxing in acetone) were not successful but instead lead to the decomposition of **9** with no formation of **10** or **11**.

Complexes **10** and **11** were isolated as red-orange solids that are soluble in polar solvents such as acetone and CH_2Cl_2 but insoluble in hexane or diethyl ether. Purification of **10** and **11** proved to be very difficult due to their tendency to oil out of solution upon attempted recrystallization. This problem was eventually overcome by slow recrystallization by layering diethyl ether over a solution of **10** or **11** in a minimum amount of acetone at low temperature (*ca.* −10 °C).

The IR spectra of **10** and **11** in CH_2Cl_2 exhibited a strong broad band at 1624 cm^{-1} and 1640 cm^{-1} respectively which was assigned to ν(NN). Both assignments were confirmed by ^{15}N isotopic substitution at N_α of the diazenido ligand whereupon significant shifts to lower wavenumbers were observed for both **10** [$\Delta\nu$(NN) = 13 cm^{-1}] and **11** [$\Delta\nu$(NN) = 16 cm^{-1}]. As with the bis-acetonitrile complex **9**, the magnitude of the shifts due to isotopic labeling in **10** and **11** were smaller than expected. The reason once again manifests itself in the IR bands assigned to ν(CC) of the aromatic ring of the aryldiazenido ligand. For unlabeled **10**, ν(NN) is 1624 cm^{-1} and ν(CC) are 1591 and 1570 cm^{-1} respectively. The labeled complex exhibited an isotopic shift to 1611 cm^{-1} for ν(NN) and a shift to 1580 and 1559 cm^{-1} for ν(CC). For unlabeled **11**, ν(NN) is 1640 cm^{-1} and ν(CC) are 1593 and 1572 cm^{-1} respectively. The labeled complex demonstrated an isotopic shift to 1624 cm^{-1} for ν(NN) and a shift to 1587 and 1566 cm^{-1} for ν(CC). These results are again consistent with significant coupling of the ν(NN) and ν(CC) vibrations in **10** and **11**.

In the ^1H NMR spectra the Cp* resonance for **10** and **11** appeared as a singlet rather than the expected triplet if the Cp* methyls are observably coupled to two equivalent phosphorus ligands. The expected J_{P-H} couplings are believed to be too small to be observed here (as was also the case for complexes **4**, **5**, and **6**). The aryldiazenido ligand in **11** gave the usual AA'BB' coupling pattern expected for a para-substituted aryl group; however, in **10** the ^1H NMR spectrum exhibited only a singlet for these four protons owing to a coincidental chemical shift, in much the same manner as the five aryl protons of toluene are found to be chemical shift degenerate.[30] In **10** the resonance at δ 1.77 assigned to the PMe_3 ligands was observed to be a virtual doublet integrating to 18 protons. The apparent coupling constant ($^2J_{P-H} + {}^4J_{P-H}$), given by the separation between the two outside peaks, was 9.0 Hz. Further evidence to support virtual coupling in complex **10** comes from the $^{13}C\{^1H\}$ NMR spectrum where the carbon resonance of the PMe_3 ligands also appears as a virtual doublet with a coupling constant ($^1J_{P-C} + {}^3J_{P-C}$) of 37 Hz. In **11** the ^1H NMR resonance at δ 3.80 assigned to the $P(OMe)_3$ ligands was observed to be a virtual triplet integrating to 18 protons with a coupling constant ($^3J_{P-H} + {}^5J_{P-H}$) of 11.6 Hz. This result was also corroborated by $^{13}C\{^1H\}$ NMR where the spectrum consists of a virtual triplet for the carbons of the $P(OMe)_3$ ligands with a coupling constant ($^2J_{P-C} + {}^4J_{P-C}$) of 41 Hz. The concept of virtual coupling has been well documented in the literature for square planar complexes containing two phosphine ligands.[31] Thus, it is chemically intuitive that virtual couplings should also manifest themselves in bis (phosphorus-ligand) complexes having a half-sandwich piano-stool type geometry. This has been shown to be the case, for example, for $Cp^*Ru(PMe_3)_2Cl$[32] and for trans-$Cp^*Re(PMe_3)_2(H)(Ph)$.[33] For the former complex, the ^1H and $^{13}C\{^1H\}$ NMR spectra show a virtual triplet while a virtual doublet is seen for the latter complex for the PMe_3 protons or carbons respectively.

It was first shown by Musher and Corey[34] that the virtual coupling pattern is dependent on the strength of the phosphorus-phosphorus coupling. That is, a small

(30) Silverstein, R. M.; Bassler, G. C.; Morrill, T. C. In *Spectroscopic Identification of Organic Compounds*; John-Wiley: New York, 1981; Chapter 4.
(31) Muetterties, E. A. In *Transition Metal Hydrides*; M. Dekker: New York, 1971; p 85.
(32) (a) Tilley, T. D.; Grubbs, R. H.; Bercaw, J. E. *Organometallics* **1984**, *3*, 274. (b) Straus, D. A.; Grumbine, S. D.; Tilley, T. D. *J. Am. Chem. Soc.* **1990**, *112*, 7801.
(33) Bergman, R. G.; Seidler, P. F.; Wenzel, T. T. *J. Am. Chem. Soc.* **1985**, *107*, 4358.
(34) Musher, J. I.; Corey, E. J. *Tetrahedron* **1962**, *18*, 791.

P–P coupling gives rise to a virtual doublet while a large P–P coupling results in a virtual triplet. Using a square planar complex of palladium, trans-$PdI_2(PMe_2Ph)_2$, Jenkins and Shaw[35] showed that the methyl resonance appeared as a virtual triplet while in the cis complex the methyl resonance was observed as a virtual doublet. These results were obtained because J_{P-P} (trans) > J_{P-P} (cis).[36] It is of interest to note that complexes **10** and **11** give rise to both extremes of virtual coupling. Complex **10** exhibits an NMR resonance which is a virtual doublet for the PMe_3 ligand while complex **11** shows a virtual triplet for $P(OMe)_3$. As follows from the preceding discussion, this result suggests that the P–P coupling between the two $P(OMe)_3$ ligands is larger than the P–P coupling between the two PMe_3 ligands. Without any information from X-ray crystal structures, and thus with caution, we suggest that this result may provide stereochemical information with respect to the relative orientations of the phosphorus ligands. Thus, it is suggested that the P–Re–P bond angle in **10** approaches 90° (corresponding to the phosphorus arrangement in Jenkins and Shaw's cis square planar complex) while the P–Re–P bond angle in **11** may open up to an angle significantly larger than 90°.

For both **10** and **11** the $^{31}P\{^1H\}$ NMR spectra displayed a single resonance at room temperature in the normal region for a coordinated phosphine or phosphite. Other than the virtual couplings for the phosphorus ligands already mentioned, the $^{13}C\{^1H\}$ NMR spectra recorded for **10** and **11** showed no atypical resonances. FAB mass spectra showed the unfragmented cation as the molecular peak for both **10** and **11**. A fragment corresponding to loss of one PMe_3 ligand was observed for **10**. No fragments were observed for **11**.

4. X-ray Structure of [Cp*Re(CO)(PMe_3)(*p*-$N_2C_6H_4OMe$)][BF_4] (3). The structure was solved with the intention of determining (i) how the geometrical details of this structure compare to previously determined rhenium aryldiazenido structures[37,38] (ii) the specific orientation or conformation adopted by the aryldiazenido ligand for a comparison with the solution behavior to be discussed, where chemically distinguishable structures are observed at low temperature.

The X-ray structure contains discrete molecular ions, [Cp*Re(CO)(PMe_3)(*p*-$N_2C_6H_4OMe$)]$^+$ and BF_4^-/I^- (95/5).[39a] There are no interionic separations significantly less than the sums of the appropriate pairs of van der Waals radii. A perspective view of the cation is shown in Figure 2. The important metrical details of the structure are given in Table 4.

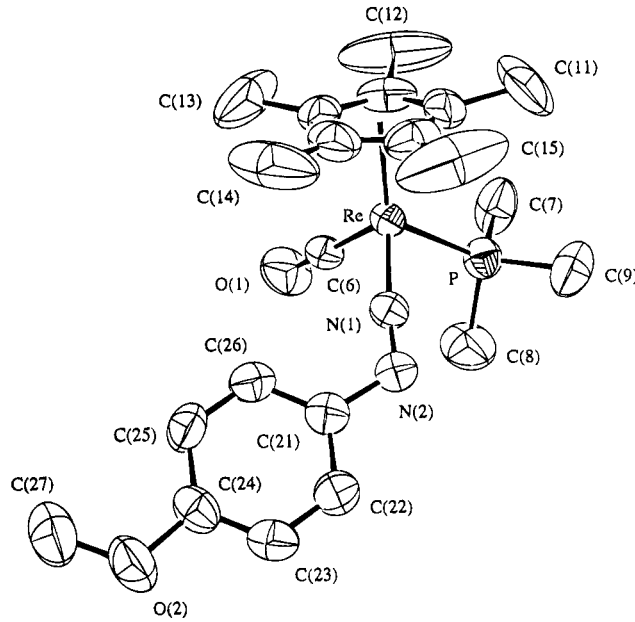

Figure 2. Perspective view of the structure of the cation [Cp*Re(CO)(PMe_3)(*p*-$N_2C_6H_4OMe$)]$^+$ in **3**. Vibrational ellipsoids are drawn at the 50% probability level.

Table 4. Selected Intramolecular Distances (Å) and Angles (deg) for [Cp*Re(CO)(PMe_3)(*p*-$N_2C_6H_4OMe$)]$^+$

Distances			
Re–P	2.388(2)	Re–C(5)	2.283(9)
Re–N(1)	1.816(6)	Re–*Cp*	1.956
Re–C(1)	2.304(9)	Re–C(6)	1.912(9)
Re–C(2)	2.286(8)	P–C(7)	1.810(12)
Re–C(3)	2.281(8)	P–C(8)	1.805(11)
Re–C(4)	2.293(10)	P–C(9)	1.792(10)
O(1)–C(6)	1.154(10)	C(3)–C(4)	1.407(13)
O(2)–C(24)	1.376(9)	C(3)–C(13)	1.497(15)
O(2)–C(27)	1.412(13)	C(4)–C(5)	1.355(15)
N(1)–N(2)	1.209(8)	C(4)–C(14)	1.491(15)
N(2)–C(21)	1.443(10)	C(5)–C(15)	1.468(14)
C(1)–C(2)	1.409(14)	C(21)–C(22)	1.394(10)
C(1)–C(5)	1.412(16)	C(21)–C(26)	1.394(11)
C(1)–C(11)	1.501(15)	C(22)–C(23)	1.329(11)
C(2)–C(3)	1.412(14)	C(23)–C(24)	1.374(13)
C(2)–C(12)	1.515(12)	C(24)–C(25)	1.401(11)
		C(25)–C(26)	1.375(12)

Angles			
N(1)–Re–P	90.3(2)	*Cp*–Re–P	125.4
C(6)–Re–P	86.7(3)	*Cp*–Re–N(1)	126.9
C(6)–Re–N(1)	93.3(3)	*Cp*–Re–C(6)	123.0
C(7)–P–Re	117.5(4)	C(9)–P–Re	115.3(4)
C(8)–P–Re	111.6(4)	C(9)–P–C(7)	105.1(5)
C(8)–P–C(7)	105.5(7)	C(9)–P–C(8)	100.0(6)
C(27)–O(2)–C(24)	118.5(8)	C(4)–C(5)–C(1)	108.7(9)
N(2)–N(1)–Re	174.7(6)	C(15)–C(5)–C(1)	128.3(13)
C(21)–N(2)–N(1)	119.1(7)	C(15)–C(5)–C(4)	122.6(14)
C(5)–C(1)–C(2)	108.5(9)	O(1)–C(6)–Re	177.4(9)
C(11)–C(1)–C(2)	125.0(15)	C(22)–C(21)–N(2)	117.2(7)
C(11)–C(1)–C(5)	126.1(14)	C(26)–C(21)–N(2)	123.8(7)
C(3)–C(2)–C(1)	105.5(8)	C(26)–C(21)–C(22)	119.0(8)
C(12)–C(2)–C(1)	125.7(14)	C(23)–C(22)–C(21)	120.7(8)
C(12)–C(2)–C(3)	127.0(14)	C(24)–C(23)–C(22)	121.3(8)
C(4)–C(3)–C(2)	109.0(9)	C(23)–C(24)–O(2)	116.6(7)
C(13)–C(3)–C(2)	123.6(14)	C(25)–C(24)–O(2)	123.8(8)
C(13)–C(3)–C(4)	127.1(14)	C(25)–C(24)–C(23)	119.6(8)
C(5)–C(4)–C(3)	108.1(9)	C(26)–C(25)–C(24)	119.2(8)
C(14)–C(4)–C(3)	125.9(14)	C(25)–C(26)–C(21)	120.0(7)
C(14)–C(4)–C(5)	125.8(14)		

[a] *Cp* denotes the center of mass of the five carbon atoms of the *Cp** ring.

The (*p*-methoxyphenyl)diazenido ligand adopts the singly-bent structure expected to be present from the ν(NN) value of 1678 cm^{-1} in the infrared spectrum and

(35) Jenkins, J. M.; Shaw, B. L. *J. Chem. Soc. A* **1966**, 1407.
(36) Garrou, P. E. *Chem. Rev.* **1981**, *81*, 229.
(37) (a) Mason, R.; Thomas, K. M.; Zubieta, J. A.; Douglas, P. G.; Galbraith, A. R.; Shaw, B. L. *J. Am. Chem. Soc.* **1974**, *96*, 260. (b) Dilworth, J. R.; Harrison, S. A.; Walton, D. R. M.; Schweda, E. *Inorg. Chem.* **1985**, *24*, 2594. (c) Chatt, J.; Fakley, M. E.; Hitchcock, P. B.; Richards, R. L.; Luong-Thi, N. T. *J. Chem. Soc., Dalton Trans.* **1982**, 345. (d) Nicholson, T.; Zubieta, J. *Inorg. Chim. Acta.* **1985**, *100*, L35. (e) Nicholson, T.; Lombardi, P.; Zubieta, J. *Polyhedron* **1987**, *6*, 1577.
(38) Barrientos-Penna, C. F.; Einstein, F. W. B.; Jones, T.; Sutton, D. *Inorg. Chem.* **1985**, *24*, 632.
(39) (a) An isostructural pair of BF_4^- and I^- salts of the rhenium complex [Cp*Re(CO)$_2$(NO)]$^+$ has been reported. See: Hubbard, J. L.; Kimball, K. L.; Burns, R. M.; Sum, V. *Inorg. Chem.* **1992**, *31*, 4224. (b) The line-width at half-peak-height for each of the ^{31}P resonances of **10** at 183 K is 69 Hz, therefore the magnitude of J_{P-P} must be significantly smaller than this value. This is consistent with the literature (see, for example, ref 50b) and with an example from our laboratory where phosphorus-phosphorus coupling has been observed. The cationic complex cis-[Cp*Re(PMe_3)$_2$(N_2)(H)][CF_3COO] has a J_{P-P} value of 48 Hz.

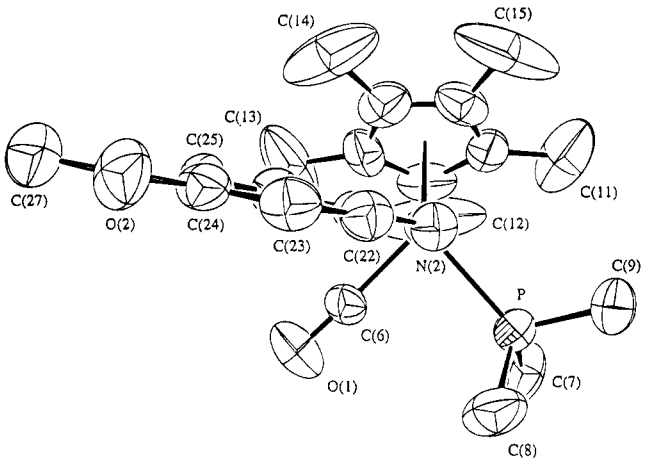

Figure 3. View of the cation $[Cp^*Re(CO)(PMe_3)(p\text{-}N_2C_6H_4OMe)]^+$ in **3** down the NNRe direction, showing the orientation of the phenyl ring.

has reasonable values for the dimensions Re–N [1.816(6) Å], N–N [1.209(8) Å], Re–N–N [174.7(6)°] and N–N–C(aryl) [119.1(7)°]. These values are comparable to those determined for other singly-bent rhenium aryldiazenido structures already published. For example, $ReCl_2(N_2Ph)(PMe_2Ph)_3$[37a] has the dimensions Re–N [1.77(2) Å], N–N [1.23(2) Å], Re–N–N [173(2)°] and N–N–C(aryl) [119(2)°] while $ReBr_2(N_2Ph)(N_2HPh)(PPh_3)_2$[37b] has the metrical details Re–N [1.793(11) Å], N–N [1.212(16) Å], Re–N–N [172.4(10)°] and N–N–C(aryl) [120.2(11)°]. Furthermore, the half-sandwich complex $CpRe(CO)(p\text{-}N_2C_6H_4Me)(AuPPh_3)$, the only other structurally determined example of a singly-bent rhenium aryldiazenido complex from our laboratory, has the following metrical values[38]: Re–N [1.78(2) Å], N–N [1.27(2) Å], Re–N–N [171(1)°] and N–N–C(aryl) [119(1)°] and a ν(NN) value of 1612 cm^{-1}. The N–N bond length in complex **3** (1.209 Å) is much shorter than typical values of N–N single bonds, which are near 1.43 Å, and thus indicates the retention of significant multiple bond character in this bond. The short Re–N bond length in complex **3** (1.816 Å) indicates that this bond has some multiple bond character as well.

The most important piece of information provided by the X-ray structure of **3** is the specific orientation of the aryldiazenido ligand relative to the other co-ligands. From Figure 2 it is clear that complex **3** has a structure in which the aryldiazenido ligand does not orient with the NNC (aryl) plane bisecting the L_1ReL_2 angle, but lies with the aryl substituent oriented towards the carbonyl ligand. This is dramatically illustrated in Figure 3 which shows a view of the cation down the NNRe direction, i.e., essentially the view of a Newman projection in this direction. In fact, the torsion angle with respect to the carbonyl co-ligand, defined by C(6)–Re–N(2)–C(21), is −56.0(4)° while the torsion angle with respect to the trimethylphosphine co-ligand represented by P–Re–N(2)–C(21) is −142.6(5)°. Furthermore, both the Re–N–N and the O–C(methoxy) fragments are approximately coplanar with the aryl ring, which suggests a degree of charge delocalization into this ring.

5. Dynamic NMR spectroscopy of Bis(phosphorus-ligand) Complexes 10 and 11. The room temperature 162 MHz $^{31}P\{^1H\}$ NMR spectrum of $[Cp^*Re(PMe_3)_2(p\text{-}N_2C_6H_4OMe)][BF_4]$ **(10)** exhibited only one trimethylphosphine resonance at δ −43.28. However, a variable temperature $^{31}P\{^1H\}$ NMR study of **10** revealed that as the temperature was lowered the single resonance began to broaden, decoalesced (192 K) and then sharpened again at 183K into two equal intensity resonances separated by a chemical shift difference ($\Delta\nu$) of 217 Hz (Figure 4). The spectrum recorded at 183 K exhibited no apparent phosphorus-phosphorus coupling. This is the expected result if each signal results from different species, each of which possesses two magnetically equivalent phosphines, but it could also be consistent with a single species with magnetically inequivalent phosphine ligands, provided that J_{P-P} is too small to be observed.[39b] The 400 MHz ^1H NMR spectrum of **10** showed no broadening of any of the proton resonances down to a temperature of 190 K.

$[Cp^*Re\{P(OMe)_3\}_2(p\text{-}N_2C_6H_4OMe)][BF_4]$ **(11)** was also investigated by variable temperature $^{31}P\{^1H\}$ NMR and results similar to **10** were obtained. At room temperature the $^{31}P\{^1H\}$ NMR of **11** showed a single resonance at δ 113.63. This began to broaden as the temperature was lowered, decoalesced at 180 K and then separated into two equal intensity broad resonances at 173 K with a chemical shift difference ($\Delta\nu$) of 1124 Hz.

For **10** and **11,** a significant chemical shift temperature dependence was noted, and the dynamic NMR processes were confirmed to be reversible for both complexes. Attempts to collect spectra below 173 K were not successful because the NMR solvent (acetone-d_6) froze at this temperature. Attempts to use a solvent of lower freezing point suitable for NMR spectroscopy such as $CDFCl_2$ also proved unsuccessful since this solvent was unable to solubilize the cationic complexes.

6. Dynamic NMR Spectroscopy of Carbonyl Phosphine and Phosphite Complexes 3–8. The room temperature $^{31}P\{^1H\}$ NMR spectrum of $[Cp^*Re(CO)(PMe_3)(p\text{-}N_2C_6H_4OMe)][BF_4]$ **(3)** exhibited a single trimethylphosphine resonance at −28.23 ppm. As the temperature was lowered the single resonance began to broaden until the signal decoalesced into two unequally populated resonances at 185 K (Figure 5) which must be assigned to the presence of two stereoisomers (δ −27.01 ppm for the major isomer and δ −27.77 ppm for the minor isomer). Integration of both resonances at the low temperature limit gave a population of 95% for the major isomer and 5% for the minor isomer.

Similar results were also obtained for the phosphite complexes, $[Cp^*Re(CO)\{P(OMe)_3\}(p\text{-}N_2C_6H_4OMe)][BF_4]$ **(7)** and $[Cp^*Re(CO)\{P(OCH_2)_3CMe\}(p\text{-}N_2C_6H_4OMe)][BF_4]$ **(8)**. At room temperature the $^{31}P\{^1H\}$ NMR of **7** showed a single resonance at 110.35 ppm. This resonance began to broaden as the temperature was lowered, decoalesced and then sharpened again into two unequal intensity resonances at 183 K assignable to two stereoisomers (δ 114.99 ppm for the major isomer and δ 116.93 ppm for the minor isomer). Integration of both resonances at the low temperature limit gave a population of 86% for the major isomer and 14% for the minor isomer. The room temperature $^{31}P\{^1H\}$ NMR of **8** also exhibited a single resonance at 104.40 ppm. The resonance began to broaden as the temperature was lowered, decoalesced and then sharpened again into two unequal intensity resonances at 183 K assignable to two stereoisomers (δ 103.40 ppm for the major isomer and δ 106.79 ppm for the minor isomer). Integration of both resonances at the low temperature limit gave a popula-

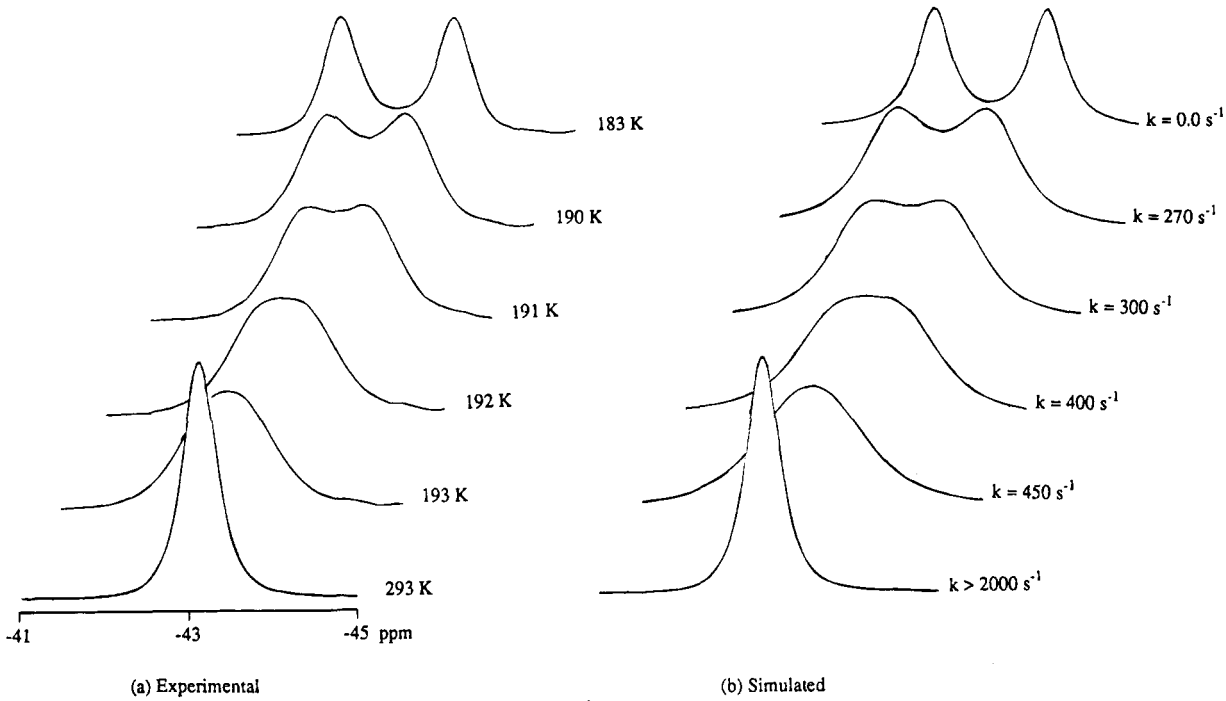

Figure 4. (a) Variable-temperature $^{31}P\{^1H\}$ NMR spectra (162 MHz) for $[Cp^*Re(PMe_3)_2(p\text{-}N_2C_6H_4OMe)][BF_4]$ **(10)**. (b) Simulated spectra.

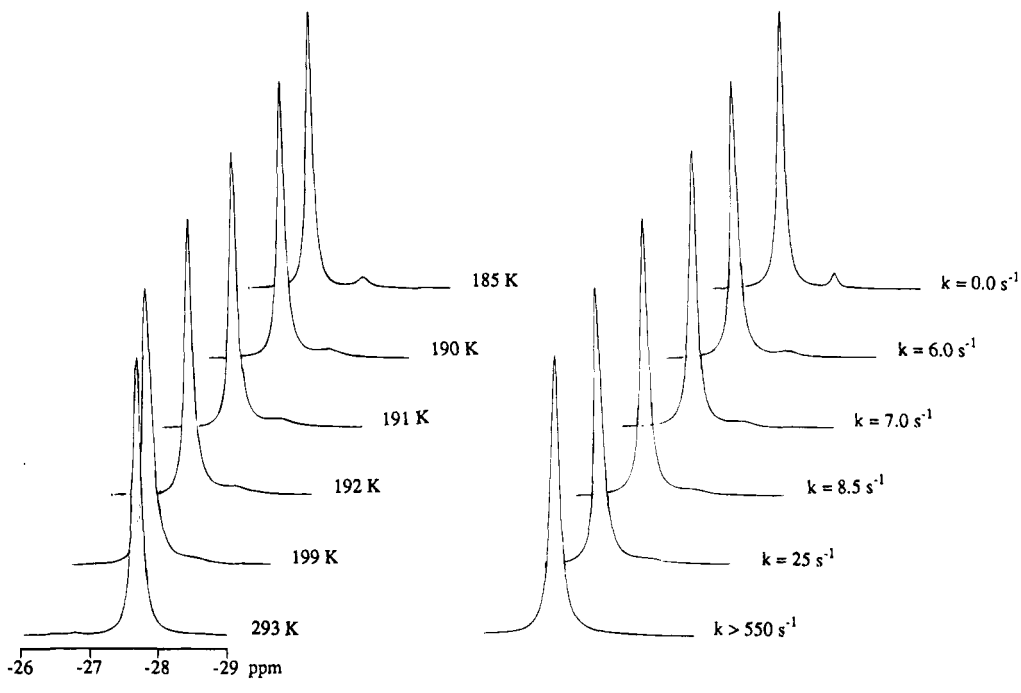

Figure 5. (a) Variable-temperature $^{31}P\{^1H\}$ NMR spectra (162 MHz) for $[Cp^*Re(CO)(PMe_3)(p\text{-}N_2C_6H_4OMe)][BF_4]$ **(3)**. (b) Simulated spectra. Rates are reported for the isomerization process from the more populated to the less populated conformer.

tion of 59% for the major isomer and 41% for the minor isomer. Once again, for **3**, **7**, and **8** a significant variation of the chemical shifts with temperature was observed, and the dynamic NMR processes were confirmed to be reversible.

Comparing the low temperature $^{31}P\{^1H\}$ spectra of complexes **3**, **7**, and **8**, it is clear that in **3** the major isomer is deshielded relative to the minor isomer while in **7** and **8** the major isomer is shielded with respect to the minor isomer.[40,41] Furthermore, the ratio of minor: major for the complexes **3**, **7**, and **8** are 1:19, 1:6.1 and 1:1.4 respectively.

A room temperature 100 MHz $^{13}C\{^1H\}$ NMR spectrum of **7** also exhibited a single resonance for the carbon of the CO ligand. This single resonance also began to broaden as the temperature was lowered and began to decoalesce at 185 K. Unfortunately, we were unable to decrease the temperature further to allow

(40) This result is most likely due to the paramagnetic component of the shielding constant which is the dominant term influencing changes in chemical shift for heavier nuclei such as phosphorus. Unfortunately, a complete understanding of the factors which contribute to the paramagnetic term has yet to be achieved.

(41) Harris, R. K. In *Nuclear Magnetic Resonance Spectroscopy*; Pitman: Massachusetts, 1983; p 185.

complete decoalescence to occur since the solution froze at 185 K. Although this experiment suggests that $^{13}C\{^1H\}$ NMR may be used to probe the isomerization process, $^{31}P\{^1H\}$ NMR is a better choice because ^{31}P is a more NMR sensitive nucleus, it can be used to monitor the isomerization process for both the carbonyl (phosphorus-ligand) complexes and bis (phosphorus-ligand) complexes, and complete decoalescence was attained within the low temperature limit of the NMR solvent (acetone-d_6).

In contrast with these results, the $^{31}P\{^1H\}$ NMR spectra of complexes **4**–**6**, where the phosphorus ligand is PEt_3, PPh_3 and PCy_3 respectively, showed the presence of only a single phosphine resonance in each case, with no evidence of broadening down to 185 K.

Discussion

1. The Aryldiazenido Ligand: Metal–Ligand Bonding and Stereochemical Preference. Although there have been numerous X-ray structure determinations of complexes with singly-bent aryldiazenido ligands[42] rather scant attention has been paid to evaluating the stereochemistry adopted by this ligand with respect to the co-ligands. That there is an electronically-driven preference is vividly illustrated by the X-ray structure of $[Cp^*Ir(C_2H_4)(N_2Ar)]^+$ (Ar = *p*-C_6H_4-OMe), where the IrNN(aryl) plane does not lie in the plane defined by the iridium and centroids of the Cp* and C_2H_4 ligands, but bisects it and thus destroys the mirror symmetry. As a consequence, the aryl group makes a closer approach to one ethylene carbon than the other.[43a] A detailed extended-Hückel molecular-orbital analysis of the phenyldiazenido ligand and its utility in understanding the stereoelectronic[44a] preference displayed in this iridium complex will be published in a future article.[43b] We do not repeat the analysis here, but proceed to apply the pertinent results to evaluate the stereoelectronic preference displayed by the aryldiazenido ligand in the structure of **3**. Related molecular orbital calculations for models of the phenyldiazenido ligand (in which, however, the important phenyl ring is only approximated by H or CH_3) have appeared previously.[8]

The *singly-bent* phenyldiazenido cationic *ligand* [43c] is reasonably represented by the valence structure **12** and the frontier orbitals are the HOMO 2a′ and LUMO 3a′ illustrated in **13** and **14** respectively. The features of these orbitals that relate to metal-ligand bond formation are illustrated in **15**. The HOMO is essentially a filled sp-hybrid σ- donor orbital, and the LUMO an empty p_π-orbital on the terminal nitrogen atom. As one would expect, this is similar to the situation for other closely related ligands such as vinylidene **16**.[44,45] Most importantly, the LUMO lies in the plane of the phenyl ring, is substantially lower in energy than the orthogonal π-antibonding orbital 3a″ that lies perpendicular to the ligand molecular plane, and is the dominant π-acceptor orbital.

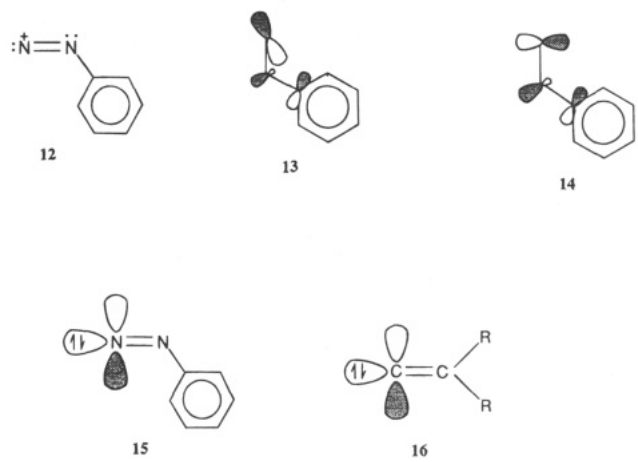

Many years ago, the frontier orbitals of the $CpML_2$ or CpMLL′ fragments were evaluated by Schilling, Hoffmann and Lichtenberger.[45a] For the d^6 symmetrical fragment Cp^*ReL_2 the HOMO is the a″ orbital shown in **17**. The overlap of this orbital with the LUMO **14** of the PhN_2^+ ligand predicts a ground-state structure in which the phenyldiazenido group lies unsymmetrically as shown in **18**, with its plane orthogonal to the mirror plane of the Cp^*ReL_2 fragment. Although no X-ray structures are available for the rhenium complexes $[Cp^*ReL_2(p\text{-}N_2C_6H_4OMe)]^+$, the structure[46] of the manganese complex $[(\eta^5\text{-}C_5H_4Me)Mn(CO)_2(o\text{-}N_2C_6H_4F)]^+$ has been determined. The Newman projection viewed down the MnNN axis (shown in Figure 6) vividly illustrates the correctness of this model.

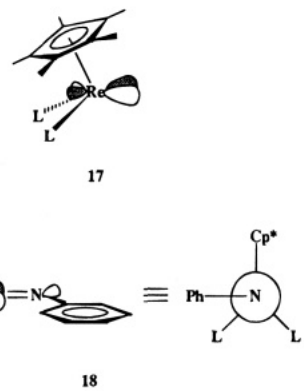

As was pointed out by Schilling, Hoffmann and Faller,[45b] when the co-ligands are inequivalent, L and L′, the symmetry is broken and the CpMLL′ fragment HOMO is reoriented. In the model example that they calculated where L = CO (a strong π-acceptor) and L′ = PH_3 (a mild donor) the plane of the HOMO for d^6 is rotated so as now to eclipse the metal-P axis in the Newman projection. In the case here, where L = CO and L′ = PMe_3 (a moderate π-acceptor), it is expected that the HOMO would lie somewhere between these extremes, and appear much as in **19**. The interaction with the PhN_2^+ LUMO **14** would then result in the plane of the phenyldiazenido ligand being tilted somewhat as in **20** or **21** with a Cp*(centroid)-Re–N–C(phenyl) dihedral angle significantly different from 90°.

(42) For a comprehensive list of structures to 1986 see: ref 3(b)

(43) (a) Einstein, F. W. B.; Yan, X.; Sutton, D. *J. Chem. Soc., Chem. Commun.* **1990**, 1466. (b) Yan, X and Sutton, D. manuscript in preparation. (c) Note that here we are considering the *singly-bent* PhN_2^+ *ligand*, not the *linear* free ion.

(44) (a) Blackburn, B. K.; Davies, S. G.; Sutton, K. H.; Whittaker, M. *Chem. Soc. Rev.* **1988**, *17*, 147. (b) Kostic, N. M.; Fenske, R. F. *Organometallics* **1982**, *1*, 974.

(45) (a) Schilling, B. E. R.; Hoffmann, R.; Lichtenberger, D. L. *J. Am. Chem. Soc.* **1979**, *101*, 585. (b) Schilling, B. E. R.; Hoffmann, R.; Faller, J. W. *J. Am. Chem. Soc.* **1979**, *101*, 592.

(46) (a) Barrientos-Penna, C. F.; Einstein, F. W. B.; Sutton, D.; Willis, A. C. *Inorg. Chem.* **1980**, *19*, 2740. (b) Barrientos-Penna, C. F.; Sutton, D. *J. Chem. Soc., Chem. Commun.* **1980**, 111.

19

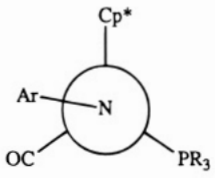

20

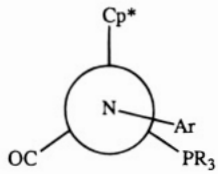

21

The stereochemistry of the rhenium-aryldiazenido fragment and its orientation with respect to the ancillary ligands Cp*, CO, and PMe_3 observed in the X-ray structure of **3** are remarkably consistent with this simple theoretical model. The phenyl ring is closely coplanar with the NNRe backbone, and is situated as shown in the Newman projection in Figure 3. The conformer observed is **20**, which is sterically less congested than **21** (which places the phenyl ring so as to nearly eclipse the PMe_3 ligand). The observed dihedral angle, as defined by Cp*(centroid)-Re−N(2)−C(21) is 82°.

An inspection of the stereochemistry of the aryldiazenido ligand as revealed by the X-ray structures of other 3-legged piano-stool complexes related to **3** indicates that these theoretically predicted types of unsymmetrical orientation of the aryldiazenido ligand commonly prevail. Examples are $(HBpz_3)Mo(CO)_2(N_2Ph)$,[47] $CpMo(CO)(PPh_3)(p\text{-}N_2C_6H_4Me)$,[48] $[CpMo(NO)(PPh_3)(p\text{-}N_2C_6H_4F)]^+$[48] and $CpRe(CO)(AuPPh_3)(p\text{-}N_2C_6H_4OMe)$.[38]

At this point it is relevant to examine the situation regarding the analogous vinylidene ligand **16**. The X-ray structure of $CpMn(CO)_2(=C=CMe_2)$[49a] shows that the plane of the vinylidene is indeed orthogonal to the $CpMn(CO)_2$ mirror plane (**22**), as expected from the orbital analysis. The cation $[CpRu(PMe_3)_2(=C=CHMe)]^+$ is similar.[49b] However, in the nitrosyl (triphenylphosphine) vinylidene complex $[CpRe(NO)(PPh_3)(=C=CHPh)]^+$, where the co-ligands are inequivalent, the plane of the vinylidene ligand is now observed[49c] to be rotated so as to more or less eclipse the Re−P vector as shown in **23**. This maximizes the overlap of the vinylidene LUMO with the rhenium d_π HOMO which is itself also rotated[45b] so as to eclipse the Re-P vector. In the X-ray structure the vinylidene substituents are found to be disposed as in **23** rather than the alternative **24**, i.e., the large phenyl substituent occupies the sterically most favored position between the small NO and medium-sized Cp ligands, and avoids eclipsing the bulky PPh_3. In numerous other papers, Gladysz has shown that this orbital analysis consistently accounts for the orientation of a range of other ligands on the rhenium nitrosyl (triphenylphosphine) fragment.[49d]

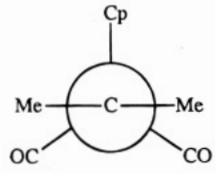

22

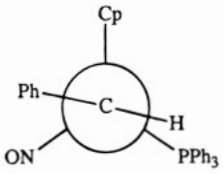

23

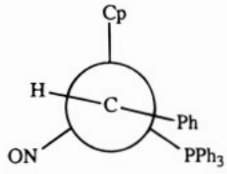

24

2. Temperature Dependence of the ^{31}P NMR Spectra for the Aryldiazenido Complexes. As described earlier, the room temperature $^{31}P\{^1H\}$ NMR spectrum of the symmetrically phosphorus-substituted complex $[Cp^*Re(PMe_3)_2(p\text{-}N_2C_6H_4OMe)][BF_4]$ **(10)** exhibited only a single phosphorus resonance. The trimethylphosphite complex **11** behaved similarly. One possible explanation for this would be a ground state structure **25** in which the PR_3 ligands are made equivalent by virtue of the aryldiazenido ligand adopting a position on the mirror plane containing the Cp* centroid and Re, and bisecting the angle subtended by the two PR_3 ligands. However, this possibility contradicts the observed X-ray structure for **3** and the molecular orbital analysis just presented, and is not consistent with the variable temperature $^{31}P\{^1H\}$ NMR spectra.

An alternative explanation which we believe to be correct is that the room temperature spectrum arises from a fast interconversion of the unsymmetrical structure illustrated in **18** with its enantiomer, as shown in Figure 1. This readily explains the variable temperature $^{31}P\{^1H\}$ NMR where at the low temperature limit two equal intensity ^{31}P resonances are observed, which can be assigned to the inequivalent phosphine or phosphite groups in configuration **18** (L = PMe_3 or $P(OMe)_3$).[50]

There are other possibilities to consider. One is interconversion of **18** with the symmetrical conformer **25**. This cannot alone be responsible for the observed temperature dependence for two reasons. First, the pathways from **25** to both **18** and its enantiomer are equivalent, so that if **25** equilibrates with **18** it also must have an equal probability of equilibrating with the enantiomer of **18** and therefore these enantiomers are themselves interconverting. Second, **25** cannot be significantly populated at the low temperature, otherwise a separate resonance for the equivalent PMe_3 ligands

(47) Avitabile, G.; Ganis, P.; Nemiroff, M. *Acta. Crystallogr., Sect. B* **1971**, *27*, 725.

(48) (a) Ferguson, G.; Ruhl, B. L.; Parvez, M.; Lalor, F. J.; Deane, M. E. *J. Organomet. Chem.* **1990**, *381*, 357. (b) Deane, M. E.; Lalor, F. J.; Ferguson, G.; Ruhl, B. L.; Parvez, M. *J. Organomet. Chem.* **1990**, *381*, 213.

(49) (a) Berke, H.; Huttner, G.; Von Seyerl, J. *J. Organomet. Chem.* **1981**, *218*, 193. (b) Bruce, M. I.; Wong, F. S.; Skelton, B. W.; White, A. H. *J. Chem. Soc., Dalton Trans.* **1982**, 2203. (c) Senn, D. R.; Wong, A.; Patton, A. T.; Marsi, M.; Strouse, C. E.; Gladysz, J. A. *J. Am. Chem. Soc.* **1988**, *10*, 6096. (d) For a recent example,see: Peng, T. S.; Pu, J.; Gladysz, J. A. *Organometallics* **1994**, *13*, 929.

(50) (a) However, each $^{31}P\{^1H\}$ resonance should appear as one half of an AB quartet. It has been mentioned in the Results section that at the lowest temperature achieved the expected P−P coupling was not observable (perhaps being obscured, since the resonances were still exchange broadened). The expected AB quartet has been observed in comparable examples, such as a related iron vinylidene complex for which J_{PP} had the value 40−50 Hz.[50b] (b) Consiglio, G.; Bangerter, F.; Darpin, C. *Organometallics* **1984**, *3*, 1446.

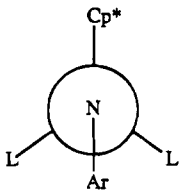

25

of **25** should be observed in addition to the two equal intensity resonances for **18**. Thus, while the interconversion of **18** and its enantiomer may possibly proceed by way of rotamer **25** (see discussion of possible mechanisms below) it is not plausible to account for the NMR behavior simply by interconversion of rotamers **18** and **25**. A second possibility (that also would readily account for the absence of P–P coupling) is that the low-temperature resonances arise from the two conformers where the plane of the aryldiazenido group lies in the mirror plane of the Cp^*ReL_2 fragment and the aryl ring is either down (**25**) or up (**26**). We consider this

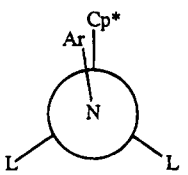

26

implausible for two reasons. First, it would be highly unlikely that these two conformers would be equally populated and give rise to the observed equal intensity resonances; secondly, molecular modelling calculations using PCMODEL[51] show that eclipsed conformations such as **26** do not correspond to minima.

To gain further insight into the isomerization process which had been established with the bis (phosphorus-ligand) complexes, the investigation was extended to include the carbonyl phosphorus-ligand complexes **3–8**. In the case of the monosubstituted complexes $[Cp^*Re(CO)(PMe_3)(p\text{-}N_2C_6H_4OMe)][BF_4]$ (**3**), $[Cp^*Re(CO)\{P(OMe)_3\}(p\text{-}N_2C_6H_4OMe)][BF_4]$ (**7**) and $[Cp^*Re(CO)\{P(OCH_2)_3CMe\}(p\text{-}N_2C_6H_4OMe)][BF_4]$ (**8**) again a single $^{31}P\{^1H\}$ NMR resonance is seen at room temperature, but the low-temperature spectrum now consists of two resonances that differ considerably in intensity (Figure 5). Precedence in the literature suggests that if there is a strong preference for one conformer in solution, the molecular conformation observed in the crystal usually dominates in solution.[52] Thus, using the PMe_3 complex **3** as an example, it is reasonable to assign the major resonance at 185 K to conformer **20** (and its enantiomer), i.e., the conformer observed in the X-ray structure. The minor conformer cannot be assigned unambiguously.[53] It could be the rotamer **25**, but since we have argued above that, for the bis-PMe_3 complex **10** this conformer cannot be significantly populated, this possibility is unlikely. More probable is that the minor resonance arises from conformer **21** (and its enantiomer). Here, the orbital interaction of the aryldiazenido group with the rhenium fragment **19** would be similar to that in **20** except that the aryldiazenido ligand is rotated by 180° (or inverted at the terminal nitrogen), thereby placing the aryl ring in a sterically less favorable position adjacent to the PMe_3 group.[54] The single $^{31}P\{^1H\}$ resonance observed at room temperature then results from rapid interconversion of diastereomers **20** and **21**. Again, the conformations where the aryldiazenido ligand eclipses either the Cp*, CO, or the PR_3 co-ligands are rejected, since they do not correspond to minima, as indicated by molecular modelling calculations using PCMODEL.[51] In principle, ^1H Nuclear Overhauser Effect (NOE) difference spectroscopy might be considered as a technique to assign the major and minor conformers in complexes **3**, **7**, and **8**. However, it is not feasible since variable temperature ^1H NMR spectroscopy indicated no apparent decoalescence of the aryl ring or ligand proton resonances into the necessary unique sets.

The differences in the minor:major isomer ratios for complexes **3**, **7**, and **8** are seen to reflect the differing steric demand of the phosphorus ligands and support assigning the major and minor isomers to **20** and **21** respectively. The ratio was found to be 1:19 for the PMe_3 complex **3**, 1:6.1 for the $P(OMe)_3$ derivative **7** and 1:1.4 for the PCage derivative **8**. The larger conformational preference shown for **3** is reduced when PMe_3 is replaced by the less sterically demanding ligand $P(OMe)_3$ and reduced further when PMe_3 is substituted by PCage (the cone angles of PMe_3, $P(OMe)_3$, and PCage are 118°, 107° and 101° respectively)[29a] and as a result the population of the minor conformer is increased for **7** and is greatest for **8**.

If interconverting diastereomers **20** and **21** are present in solution for **3** (and similarly for **7** and **8**), it might be possible to detect these by IR spectroscopy in view of its shorter timescale when compared to NMR. We carefully examined the ν(CO) and ν(NN) absorptions for **3**, **7**, and **8** both for solution (CH_2Cl_2) and solid state (KBr) room-temperature spectra, but in all cases these appeared to be single absorptions. Reasons for this could be the preponderance of one diastereomer, or small and unresolvable differences in the ν(CO) and ν(NN) values for each diastereomer.

The triethylphosphine (carbonyl), triphenylphosphine (carbonyl) and tricyclohexylphosphine (carbonyl) compounds **4**, **5**, and **6** were also investigated by variable temperature $^{31}P\{^1H\}$ NMR. Complexes **4**, **5**, and **6** were chosen because triethylphosphine (cone angle = 132°),[29a] triphenylphosphine (cone angle = 145°)[29a] and tricyclohexylphosphine (cone angle = 170°)[29a] are sterically larger ligands than PMe_3, $P(OMe)_3$, or PCage and PEt_3 and PCy_3 have similar electronic properties to PMe_3 but

(51) PCMODEL is available from Serena Software, Bloomington, IN. See: Gajewski, J. J.; Gilbert, K. E.; McKelvey, I. In *Advances in Molecular Modelling*; Liotta, D., Ed.; JAI Press: Greenwich, CT, 1990; Vol. 2, p 65.

(52) (a) Luck, L. A.; Elcesser, W. L.; Hubbard, J. L.; Bushweller, C. H. *Magn. Reson. Chem.* **1989**, *27*, 488. (b) Bushweller, C. H. *J. Am. Chem. Soc.* **1969**, *91*, 1968. (c) Jensen, F. R.; Bushweller, C. H. *J. Am. Chem. Soc.* **1969**, *91*, 3223. (d) Bushweller, C. H.; Golini, J.; Rao, G. U.; O'Neil, J. W. *J. Am. Chem. Soc.* **1970**, *92*, 3055. (e) Bushweller, C. H.; O'Neil, J. W.; Halford, M. H.; Bissett, F. H. *J. Am. Chem. Soc.* **1971**, *93*, 1471.

(53) The results from the dynamic $^{31}P\{^1H\}$ NMR study of **3**, **7** and **8** indicate the presence of two diastereomers, where each diastereomer is responsible for one $^{31}P\{^1H\}$ resonance at 185 K. Each diastereomer is actually comprised of two enantiomers, arising from chirality at Re, which are indistinguishable from each other by NMR spectroscopy. Formation of the enantiomers arises from the method of synthesis, i.e., there is equal probability of removing either one of the two carbonyl co-ligands in complex **1** during the synthesis of complexes **3–8**.

(54) In the case of the vinylidene complex $[CpRe(NO)(PPh_3)(=C=CHPh)]^+$ analogous conformers are proposed for two *isolable* geometric isomers, which are present at equilibrium in solution in a 4:1 ratio. See: ref 49c.

varying size. Variable temperature $^{31}P\{^1H\}$ NMR of **4**, **5**, and **6** indicated no decoalescence of the single phosphorus resonance observed at room temperature even down to *ca.* 183 K.

To summarize, the bis(phosphorus-ligand) complexes $[Cp^*Re(PR_3)_2(p\text{-}N_2C_6H_4OMe)]^+$ could be synthesized for PMe_3 (**10**) and $P(OMe)_3$ (**11**) but not for the more bulky ligands PPh_3 or PCy_3, and in both cases decoalescence of the $^{31}P\{^1H\}$ NMR spectra could be obtained. The carbonyl phosphorus-ligand complexes $[Cp^*Re(CO)(PR_3)(p\text{-}N_2C_6H_4OMe)]^+$ could be synthesized for all the phosphines and phosphites attempted, i.e., PMe_3 (**3**), PEt_3 (**4**), PPh_3 (**5**), PCy_3 (**6**), $P(OMe)_3$ (**7**) and PCage (**8**). Each of these complexes exhibited a single $^{31}P\{^1H\}$ resonance at room temperature but only for the ones with the smallest cone angle, i.e., **3**, **7**, and **8**, could separate low-temperature resonances for the major and minor stereoisomers be observed. The failure to observe this in the case of the remainder could possibly be due to a lower temperature of decoalescence in these cases. However, as is clearly illustrated by the minor:major isomer ratios from the low-temperature $^{31}P\{^1H\}$ NMR spectra for **3**, **7**, and **8**, the population of the minor conformer decreases as the cone angle of the phosphorus ligand increases on going from PCage to $P(OMe)_3$ to PMe_3. Therefore, it is more likely that in the remainder the crowded conformer **21** is not significantly populated and the observed resonance is essentially that of the uncrowded conformer **20**.

Interestingly, the variable temperature $^{13}C\{^1H\}$ NMR of the dicarbonyl complex $[Cp^*Re(CO)_2(p\text{-}N_2C_6H_4OMe)][BF_4]$ **1**, which exhibits a single carbonyl resonance at room temperature, showed no decoalescence of the carbonyl signal even down to a temperature of 173 K. Unlike complexes **3**–**8** which have a sterically demanding phosphorus co-ligand, the two carbonyl co-ligands of complex **1** offer little if any steric contribution to the orientation of the aryldiazenido substituent. Although no X-ray structure of **1** has been completed, it was pointed out above that the structure of the related Mn complex $[(\eta^5\text{-}C_5H_4Me)Mn(CO)_2(o\text{-}N_2C_6H_4F)][BF_4]$ shows that the two CO groups are indeed inequivalent as a result of the unsymmetrical orientation of the aryldiazenido group (Figure 6).[46] The rhenium complex **1** is expected to be entirely similar. Furthermore, as will be addressed in the discussion which follows, the activation barriers for conformational isomerization of the aryldiazenido ligand are larger for complexes whose ligands are good σ-electron-donors and poor π-electron-acceptors (i.e. **10** > **11** and **3** > **7** or **8**). With this in mind we believe that the room temperature $^{13}C\{^1H\}$ NMR spectrum of **1** arises from a fast interconversion (Figure 1) of the unsymmetrical structure illustrated in **18** (L = CO) with its enantiomer (as was postulated for complexes **10** and **11**) and that the static spectrum is not achieved even at 173 K perhaps because of a small ^{13}C chemical shift difference in the individual CO resonances or more likely as a result of a very low activation barrier.[55,56]

3. Activation Barriers for Conformational Isomerization of the Aryldiazenido Ligand. From the dynamic $^{31}P\{^1H\}$ NMR investigation, the activation barriers for the isomerization of the aryldiazenido ligand in complexes **3**, **7**, **8**, **10**, and **11** were determined and

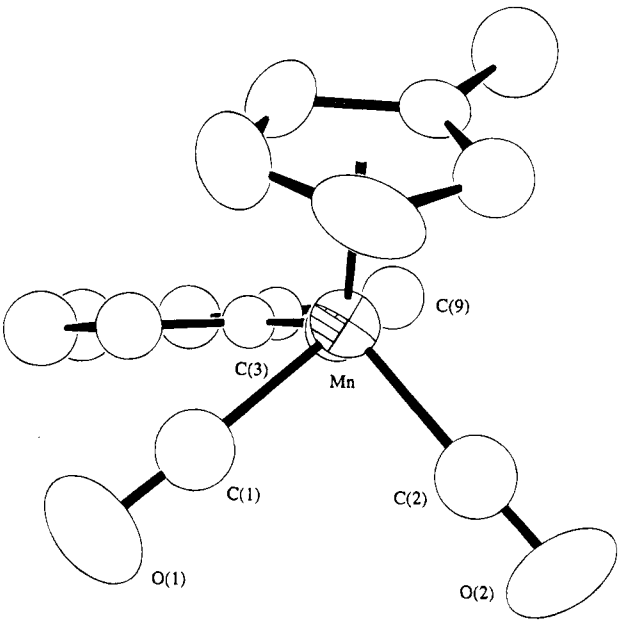

Figure 6. View of the cation $[(MeC_5H_4)Mn(CO)_2(o\text{-}N_2C_6H_4F)][BF_4]$ down the NNMn direction, showing the orientation of the phenyl ring. Vibrational ellipsoids are drawn at the 50% probability level.

Table 5. Activation Parameters for Isomerization of the Aryldiazenido Ligand

complex	$\Delta G^\ddagger$ (kJ/mol)	$\Delta H^\ddagger$ (kJ/mol)	$\Delta S^\ddagger$ (J/(mol·K))	E_a (kJ/mol)	A ($\times 10^{13}$)
3[a,c]	43.0 ± 0.4	46.5 ± 0.6	18.5 ± 2.8	48.2 ± 0.6	11.0 ± 8.0
3[b,c]	38.4 ± 0.4	40.7 ± 1.0	12.5 ± 4.6	42.4 ± 0.8	5.3 ± 2.6
7[a,c]	41.2 ± 0.4	44.3 ± 1.0	16.7 ± 5.6	46.0 ± 1.2	8.5 ± 4.8
7[b,c]	38.3 ± 0.4	41.4 ± 2.0	16.6 ± 10.2	43.0 ± 2.0	8.4 ± 8.0
8[a,c]	39.2 ± 0.6	43.0 ± 1.5	23.1 ± 7.4	44.7 ± 1.5	19.0 ± 8.0
10[c]	37.0 ± 0.6	47.3 ± 2.2	54.1 ± 18.0	48.9 ± 2.2	730 ± 720
10[d]	36.5 ± 0.4				
11[c,e]	31.4 ± 0.4	39.4 ± 2.4	42.3 ± 16.2	41.0 ± 2.4	180 ± 200
11[d,e]	31.6 ± 0.4				

[a] For the isomerization process from the more populated to the less populated conformer. [b] For the isomerization process from the less populated to the more populated conformer. [c] Values for $\Delta G^\ddagger$ are given for a temperature of 190 K. [d] Values for $\Delta G^\ddagger$ are given for the respective coalescence temperatures, which are 192 K for **10** and 180 K for **11**. [e] Data for **11** are considered to be less reliable than the remainder because the coalescence temperature approaches the lowest accessible temperature, making it possible only to estimate the stopped-exchange peak separation $\Delta\nu$. This uncertainty is not factored into the calculated errors.

are summarized in Table 5. Values of $\Delta G^\ddagger$ for the bis(phosphorus-ligand) complexes **10** and **11** were determined initially at the respective coalescence temperatures. For the bis-PMe_3 complex **10**, $\Delta G^\ddagger_{Tc}$ was calculated to be 36.5 ± 0.4 kJ/mol at 192 K while a value for $\Delta G^\ddagger_{Tc}$ of 31.6 ± 0.4 kJ/mol at 180 K was determined for the bis-$P(OMe)_3$ complex **11**. This result indicates that the barrier to isomerization of the aryldiazenido ligand is raised when the co-ligands are both trimethylphosphine instead of trimethylphosphite. This statement is made with caution since it is recognized that the $\Delta G^\ddagger_{Tc}$ values for complexes **10** and **11** were calculated at different coalescence temperatures. However, these activation energy values for **10** and **11** are sufficiently different that a qualitative comparison is still likely to

(55) A similar explanation probably accounts for the apparently equivalent MeCN ligands in the NMR spectra of **9**.

(56) The CO groups are also inequivalent in the X-ray structure of the methyldiazenido complex $CpW(CO)_2(N_2Me)$; only a single ^{13}CO resonance is reported in the ambient temperature ^{13}C NMR spectrum. See: (a) Herrmann, W. A.; Biersack, H. *Chem. Ber.* **1977**, *110*, 896. (b) Hillhouse, G. L.; Haymore, B. L.; Herrmann, W. A. *Inorg. Chem.* **1979**, *18*, 2423.

Table 6. Comparison of ΔG° Values Determined from Line Shape Analysis and from Equilibrium Populations

complex	temperature (K)	ΔG° (kJ/mol)
3[a]	190	4.6 ± 0.8
3[b]	190	4.7 ± 0.8
7[a]	190	2.9 ± 0.8
7[b]	190	2.9 ± 0.8
8[a]	190	0.6 ± 1.2
8[b]	190	0.6 ± 1.2

[a] From line shape analysis. [b] From equilibrium populations.

be meaningful.[57] The line-shape analysis substantiates this. The observed and simulated spectra for **10** are shown in Figure 4. For the bis-PMe_3 complex **10**, $\Delta G^\ddagger_{190}$ was calculated to be 37.0 ± 0.6 kJ/mol, while for the bis-$P(OMe)_3$ complex **11**, $\Delta G^\ddagger_{190}$ was 31.4 ± 0.4 kJ/mol. These values are consistent, within experimental error, with the activation energies calculated for **10** and **11** using the temperature of coalescence approximation and taken together these results indicate that the activation barrier is raised by *ca.* 5 kJ upon substituting $P(OMe)_3$ by PMe_3.

For complexes **3**, **7**, and **8** where the interconverting diastereomers have unequal populations, the rate constants were determined from the lineshape analysis for the interconversion from the more populated conformer to the less populated conformer, and for the reverse direction (Table 1). The observed and simulated spectra for **3** are shown in Figure 5. The values of $\Delta G^\ddagger$ for the isomerization process (major isomer to minor isomer) for the carbonyl phosphine and phosphite complexes **3**, **7**, and **8** were found to be 43.0 ± 0.4, 41.2 ± 0.4 and 39.2 ± 0.6 kJ/mol respectively at 190 K. The trimethylphosphine ligand again evidently causes a small increase in the activation barrier compared with either phosphite, but less than the *ca.* 5 kJ difference observed for the bis-trimethylphosphine and bis-trimethylphosphite complexes **10** and **11** at the same temperature. The data, though limited, indicate a higher barrier for the better σ-donor (and poorer π-acceptor) PMe_3 ligand.

The two unequally populated ground-state conformers in **3**, **7**, or **8** give rise to two different values of $\Delta G^\ddagger$ for the interconversion process which correspond to the kinetic barriers for conversion of major to minor isomer and for minor to major isomer. The difference in $\Delta G^\ddagger$ for these forward and reverse interconversions equals ΔG°. The ΔG° value obtained in this fashion was then compared to the ΔG° value determined from the relative populations of the major and minor isomers at the low temperature limit and these were found to be in complete agreement within experimental error (Table 6). This indicates that the ratio of isomers did not change significantly over the temperature range during which coalescence occurred, an assumption that is made in calculating simulated spectra in *DNMR3*.

It is apparent that the entropy of activation terms ($\Delta S^\ddagger$) for the interconversion process are of comparable magnitudes, and are small positive values, indicative of an intramolecular exchange.[58] Several reliable examples of positive values for $\Delta S^\ddagger$ have been reported in the literature for intramolecular processes in organometallic complexes.[59] It is believed that different interactions with the solvent in the ground and excited states is responsible for these positive entropy of activation values.[60] If the transition state is significantly less polar than the ground state then interactions with polar solvent molecules will be diminished, resulting in a decreased order in the solvent cage around the molecule in the transition state and thus an appreciable positive value for $\Delta S^\ddagger$.

The variation of the $^{31}P\{^1H\}$ NMR chemical shift with temperature for complexes **3**, **7**, **8**, **10**, and **11** was mentioned previously. The temperature dependence of chemical shifts in the literature has been explained in terms of changes in fast rotamer equilibria and in solute-solute and/or solute-solvent interactions.[61] The positive values for $\Delta S^\ddagger$ and the considerable temperature dependence observed here are therefore consistent with solvent (acetone-d_6) interactions with these complexes and the positive $\Delta S^\ddagger$ values are indicative of fewer solvent-complex interactions in the transition state. To justify this explanation for positive $\Delta S^\ddagger$ values requires the solvent-dependence of the variable temperature $^{31}P\{^1H\}$ NMR to be studied, especially using a non-polar solvent. Unfortunately, these are all cationic complexes and are not soluble in non-polar solvents. To conclude, although the $\Delta S^\ddagger$ values support an intramolecular exchange process, they do not distinguish between different possible intramolecular mechanisms for isomerization.

Further support for an intramolecular isomerization process is provided by a series of competition experiments. Complex **3**, $[Cp^*Re(CO)(PMe_3)(p\text{-}N_2C_6H_4OMe)][BF_4]$, was examined in acetone-d_6 for dissociative exchange in the presence of excess $P(OMe)_3$ by ^1H NMR. A spectrum of this solution acquired after 24 h indicated no substitution of PMe_3 in **3** by $P(OMe)_3$. Furthermore, the ^1H NMR spectrum obtained after this solution was refluxed for 4 h, also showed only the resonances corresponding to complex **3** and excess trimethylphosphite. Analogous results were obtained when this procedure was repeated for $[Cp^*Re(CO)\{P(OMe)_3\}(p\text{-}N_2C_6H_4OMe)][BF_4]$ (**7**) in the presence of excess PMe_3.

4. Conformational Isomerization of the Aryldiazenido Ligand. Despite the numerous singly-bent aryldiazenido-ligand complexes that have been synthesized and characterized, there has been remarkably little note taken of whether the aryldiazenido ligand adopts a rigid structure and orientation with respect to the co-ligands, or whether it readily undergoes some kind of rearrangement. Indeed, there are very few cases where the reported data allow examination of this feature. For example, it has been mentioned that the CO groups are inequivalent in the X-ray structure of $[(\eta^5\text{-}C_5H_4Me)Mn(CO)_2(o\text{-}N_2C_6H_4F)]^+$ as a result of the orientation of the aryldiazenido ligand, yet whether or not the expected two ^{13}CO resonances occur is not known since the ^{13}C NMR spectrum has not been reported.[46, 56] The bis (phenyldiazenido) complex [(acac)-

(57) Binsch, G. In *Dynamic Nuclear Magnetic Resonance Spectroscopy*; Jackman, L. M., Cotton, F. A., Eds.; Academic Press: New York, 1975; Chapter 3.

(58) (a) Lindner, E.; Mockel, A.; Mayer, H. A.; Kuhbauch, H.; Fawzi, R.; Steimann, M. *Inorg. Chem.* **1993**, *32*, 1266. (b) Koe, J. R.; Tobita, H.; Suzuki, T.; Ogino, H. *Organometallics* **1992**, *11*, 150.

(59) (a) Howe, J. J.; Pinnavaia, T. J. *J. Am. Chem. Soc.* **1970**, *92*, 7342. (b) Pinnavaia, T. J.; Lott, A. L. *Inorg. Chem.* **1971**, *10*, 1388. (c) Hutchison, J. R.; Gordon, J. G.; Holm, R. H. *Inorg. Chem.* **1971**, *10*, 1004. (d) Case, D. A.; Pinnavaia, T. J. *Inorg. Chem.* **1971**, *10*, 482.

(60) (a) Berg, U.; Sjöstrand, U. *Org. Magnet. Res.* **1978**, *11*, 555. (b) Sandstrom, J. *Dynamic NMR Spectroscopy*; Academic Press: London, 1982; Chapter 7.

(61) (a) Harris, R. K. In *Nuclear Magnetic Resonance Spectroscopy*; Pitman: Massachusetts, 1983; p 201. (b) Sandström, J. *Dynamic NMR Spectroscopy*; Academic Press: London, 1982; Chapter 6. (c) Berg, U.; Sandström, J.; Jennings, W. B.; Randall, D. *J. Chem. Soc., Perkin II* **1980**, 949; *Tetrahedron Lett.* **1976**, 3197.

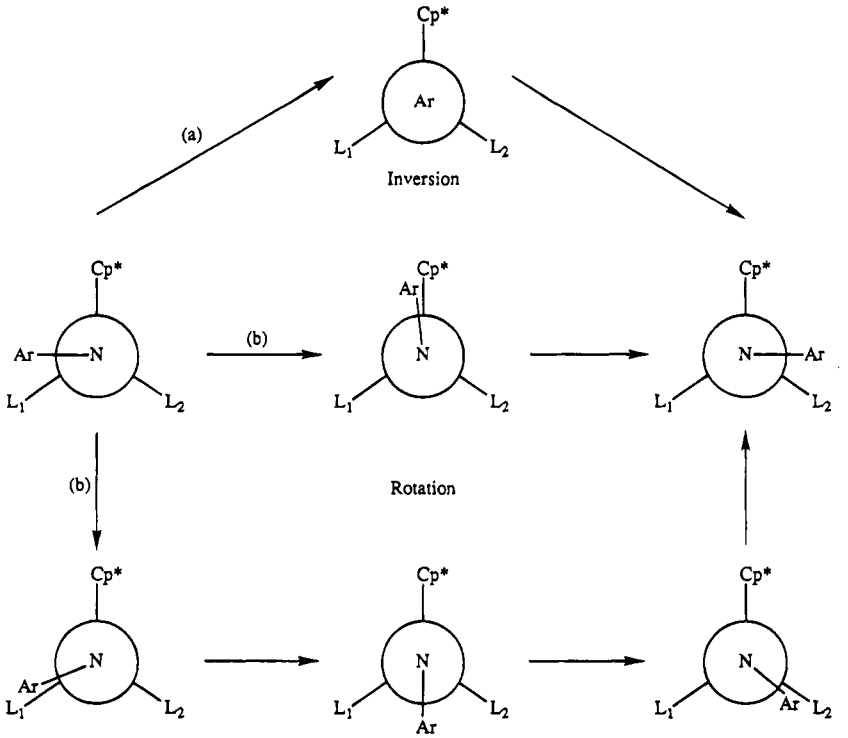

Figure 7. Plausible mechanistic pathways for the conformational isomerization of the aryldiazenido ligand. (a) sp^2 nitrogen inversion at N_β. (b) restricted rotation around the Re–N–N axis.

$Mo(OCH_3)(N_2C_6H_5)_2]_2$ (acac = acetylacetonato) has been isolated and crystallographically characterized in two isomeric forms in which two of the N_2Ph ligands are mutually either syn or anti. These isomers interconvert in solution, and a conformational isomerization of the phenyldiazenido ligand was suggested to be responsible. A variable temperature ^1H NMR study resulted in a value of $\Delta G^\ddagger = 57 \pm 1$ kJ mol^{-1} (at $T_c = 280$ K) for the activation barrier. It was suggested that this value was in the region of the barrier for restricted rotation about a partial double bond.[62] Isomers resulting from bis (aryldiazenido) ligands have been discussed in other cases.[63] We have also found some instances where stereochemical non-rigidity of the angular singly-bent aryldiazenido ligand seems to have been automatically assumed (though not commented upon) in interpreting solution NMR data. In one example, there are more equivalent Mo and oxo sites by ^{95}Mo and ^{17}O NMR in $[Mo_6O_{18}(NNPh)]^{3-}$ than the static structure would predict.[64] In another, although there is no plane of symmetry equating equatorial dimethyldithiocarbamate (dtc) ligands in the X-ray structure of $[Mo(dtc)_3(N_2Ph)]$, nevertheless these methyl groups are pairwise equivalent in the room temperature NMR spectrum.[65] For the compounds in this study, we have been able to obtain direct NMR evidence for the stereochemical non-rigidity of the aryldiazenido group and have been able to observe the slowed-exchange conditions in particular examples.

The two possible mechanisms that must be considered for the conformational isomerization of the aryldiazenido ligand are (i) a restricted rotation around the Re–N–N axis, or (ii) an sp^2 nitrogen inversion at N_β, sometimes called a lateral shift mechanism. These are illustrated in Figure 7. Even in the evidently much simpler cases of organic Schiff bases or imines $R_2C{=}NPh$ the prevailing mechanism of isomerization has been much debated.[66] For an unactivated imine such as $Me_2C{=}NPh$, $\Delta G^\ddagger$ is about 21 kcal mol^{-1} (88 kJ mol^{-1}).[67] This corresponds reasonably well to the calculated barrier for a lateral shift mechanism, whereas that for rotation about the C=N double bond is about twice as large.[68] It therefore seems to be generally thought that the lateral shift mechanism operates in simple unactivated imines. However, the presence of substituent heteroatoms on the imino carbon atom can lower the barrier dramatically, and rotation about the C=N bond (of reduced bond-order) becomes dominant.[66] Conversely, the presence of a phenyl group on the imino nitrogen is expected to act to stabilize the transition state for the lateral shift mechanism.[66] Phenyl-substituted vinylidene (M=C=CHPh) and linear azavinylidene (M=N=CHPh) ligands are interesting systems with which to compare the barrier for the singly-bent phenyldiazenido ligand (M=N=NPh). In these, of course, it would appear that rotation is the only possible isomerization mechanism (but see subsequent discussion of azavinylidene). The barrier in the Gladysz rhenium vinylidene complex $[CpRe(NO)(PPh_3)(=C{=}C\text{-}HPh)]^+$ ($\Delta G^\ddagger = 22$ kcal at 25 °C) is very similar to that for the corresponding alkylidene complex $[CpRe(NO)(PPh_3)(=CHPh)]^+$ despite the expectation that steric hindrance to rotation of the more remote phenyl group in the former might be significantly less.[49c] As far as we are aware, this is the only vinylidene system for

(62) Carillo, D.; Gouzerh, P; Jeannin, Y. *Nouv. J. Chim.* **1985**, *9*, 749.
(63) See ref 48(a) and references cited therein.
(64) Bank, S.; Liu, S.; Shaikh, S. N.; Sun, X.; Zubieta, J.; Ellis, P. D. *Inorg. Chem.* **1988**, *27*, 3535.
(65) Bishop, E. O.; Butler, G.; Chatt, J.; Dilworth, J. R.; Leigh, G. J.; Orchard, D.; Bishop, M. W. *J. Chem. Soc., Dalton Trans.* **1978**, 1654.
(66) Jackman, L. M. In *Dynamic Nuclear Magnetic Resonance Spectroscopy*; Jackman, L. M., Cotton, F. A., Eds.; Academic Press: New York, 1975; p 244.
(67) (a) Curtin, D. Y.; Grubbs, E. J.; McCarty, C. G. *J. Am. Chem. Soc.* **1966**, *88*, 2775. (b) Marullo, N. P.; Wagener, E. H. *Tetrahedron Lett.* **1969**, 2555.
(68) (a) Raban, *J. Chem. Soc., Chem. Commun.* **1970**, 1415. (b) Lehn, J. M.; Munsch, B.; Millie, P. *Theor. Chim. Acta* **1970**, *16*, 351.

which geometric isomers have been isolated. Barriers to rotation are generally much lower in other vinylidene complexes. For example, $\Delta G^{\ddagger} = 9-10$ kcal has been estimated for [CpFe(diphosphine)(=C=CHPh)]$^{+}$.[50b] Turning to the azavinylidene ligand, the barrier has been measured recently for some tungsten hydridotris-(3,5-dimethylpyrazolylborate) (Tp′) complexes Tp′W-$(CO)_2$(=N=CHR).[69] For R = *n*-Pr, a value of $\Delta G^{\ddagger} = 9.6$ kcal at −80 °C was obtained, but for the complex with R = Ph the barrier is presumably smaller since, while spectral broadening was observed, decoalescence could not be achieved down to -105 °C. A low barrier, and consequently only averaged NMR spectra, has been reported for other azavinylidene complexes.[70,71] It has been suggested that low barriers may be the result of isomerization of the azavinylidene ligand to a non-linear structure in which the nitrogen is sp^2-hybridized.[70] However, the barrier in Cp_2ZrCl(=N=CHPh) may be very high, since geometric isomerization could not be achieved thermally or photochemically.[70]

It is clear from the above comparisons that even the rotational barriers for linear metallocumulene ligands of this type can cover a wide range, and show significant dependence on such variables as the metal, its *d*-electron configuration and row in the periodic table, the number and nature of the co-ligands, and the geometry of the complex. Therefore, with only the limited data that we have presently accumulated in this study for the much more complex case of the aryldiazenido ligand, it would be premature to venture an opinion at this time on whether this ligand isomerizes by way of rotation or inversion in these rhenium compounds. Nevertheless, it is notable that the barriers we observe are extremely low in comparison to the closest analog presently available, i. e., the *rotation* barrier for the Gladysz rhenium nitrosyl vinylidene complex.[49c] Work is presently underway in our laboratory to extend this investigation to a wider range of aryldiazenido complexes and their derivatives with the aim of accumulating data that may allow us to distinguish the mechanism that is operating in appropriate examples.

(69) Powell, K. R.; Perez, P. J.; Luan, L.; Feng, S. G.; White, P. S.; Brookhart, M.; Templeton, J. L. *Organometallics* **1994**, *13*, 1851.
(70) Erker, G.; Fromberg, W.; Kruger, C.; Raabe, E. *J. Am.Chem.Soc.* **1988**, *110*, 2400.
(71) Dormond, A.; Aaliti, A.; Elbouadili, A.; Moise, C. *J. Organomet. Chem.* **1987**, *329*, 187.

Conclusion

In this paper we have demonstrated that the rhenium half-sandwich complexes $[(\eta^5\text{-}C_5Me_5)ReL_1L_2(p\text{-}N_2C_6H_4\text{-}OMe)]^+$ (where (a) $L_1 = L_2 = CO$ **(1)**, PMe_3 **(10)** or $P(OMe)_3$ **(11)** and (b) $L_1 = CO$; $L_2 = PMe_3$ **(3)**, PEt_3 **(4)**, PPh_3 **(5)** (where Ph = C_6H_5), PCy_3 **(6)** (where Cy = C_6H_{11}), $P(OMe)_3$ **(7)**, or PCage **(8)** (where PCage = $P(OCH_2)_3CMe$)) have ground state structures in which the aryl ring of the singly-bent aryldiazenido ligand orients with its molecular plane orthogonal to the plane bisecting the L_1ReL_2 angle. This conformational preference was predicted from the results of simple EHMO considerations and corroborated by a variable temperature ^1H, $^{31}P\{^1H\}$ and $^{13}C\{^1H\}$ NMR study of complexes **1**, **3**−**8**, **10**, **11** and by an X-ray structural analysis of complex **3**. Furthermore, the aryldiazenido ligand is capable of undergoing a conformational isomerization which interconverts the conformer in which the aryl group is oriented towards L_1 with its partner in which it is oriented towards L_2. The relative populations of the two conformers have been examined in selected examples, and the barriers to isomerization have been measured.

Acknowledgment. We thank NSERC Canada for supporting this work through operating and infrastructure grants to DS and FWBE. We also thank Dr. Xaioqian Yan for suggesting this investigation, for providing Figure 6 and the results of EHMO calculations, and for numerous enlightening discussions; and Dr. John D'Auria for use of the XRF instrument and for technical assistance.

Supplementary Material Available: Tables of supplementary crystallographic data, atomic coordinates and temperature factors, bond lengths and angles, and selected intramolecular torsion angles and least-squares planes for complex **3** and text giving detailed syntheses of complexes **1**−**8** (12 pages). Ordering information is given on any current masthead page.

OM940568E